

**SPECTROMETRIC STUDY OF STELLAR  
OBJECTS**

**By**

**Janaka Adassuriya**

Dissertation submitted in partial fulfillment of the requirements for the  
**BACHLOR OF SCIENCE SPECIAL DEGREE IN PHYSICS**

**of the**

**UNIVERSITY OF COLOMBO**

**SRI LANKA**

**December 2001**

# CONTENTS

|   | <b>Page</b> |
|---|-------------|
| <b>Chapter 1 – INTRODUCTION</b>   | <b>1</b>    |
| <b>1.1 Application of Spectroscopy</b>  |             |
| 1.1.1 Discovery of Expansion of the Universe  | <b>3</b>    |
| 1.1.2 Discovery of Sodium in Mercury's thin Atmosphere                              | <b>5</b>    |
| 1.1.3 The use of Doppler Effect to Measure the Period<br>of the Rotation of the Sun | <b>6</b>    |
| <b>Chapter 2 – INSTRUMENTATION</b>  | <b>8</b>    |
| <b>2.1 CCD Camera</b>   |             |
| 2.1.1 Operation of CCD Camera   | <b>9</b>    |
| 2.1.2 Camera Hardware Architecture  | <b>11</b>   |
| 2.1.3 CCD Cooling   | <b>12</b>   |
| 2.1.4 Quantum Efficiency of CCD   | <b>13</b>   |
| 2.1.5 Readout Noise   | <b>14</b>   |
| 2.1.6 Linearity   | <b>14</b>   |
| 2.1.7 Dark Current  | <b>14</b>   |
| <b>2.2 Spectrograph</b>   | <b>16</b>   |
| <b>Chapter 3 – EXPERIMENTAL PROCEDURE</b>   | <b>19</b>   |
| <b>3.1 Observation of Line Spectra</b>  | <b>19</b>   |
| <b>Chapter 4 – RESULT AND DATA ANALYSIS</b>   | <b>21</b>   |
| <b>4.1 Identification of Chemical Composition of Solar Spectrum</b>                 |             |
| 4.1.1 Line Identification   | <b>21</b>   |
| 4.1.2 Reference Line Matching   | <b>22</b>   |
| 4.1.3 Identification of Pixel Points of Reference Lines                             | <b>24</b>   |
| 4.1.4 Solar Spectrum (7200-7600) °A   | <b>27</b>   |
| 4.1.5 Solar Spectrum (6800-7300) °A   | <b>30</b>   |
| 4.1.6 Solar Spectrum (6200-6900) °A   | <b>33</b>   |
| 4.1.7 Solar Spectrum (5900-6200) °A   | <b>36</b>   |
| 4.1.8 Solar Spectrum (4900-5700) °A   | <b>39</b>   |
| 4.1.9 Solar Spectrum (4200-5000) °A   | <b>42</b>   |
| 4.1.10 Solar Spectrum (4100-4400) °A  | <b>46</b>   |

|   | <b>Page</b> |
|---|-------------|
| <b>4.2 Determination of Solar Temperature using<br/>Black Body Radiation Curve</b>                        | <b>49</b>   |
| 4.2.1 Identification of Intensity Distribution of entire<br>Solar Spectrum                                | <b>49</b>   |
| 4.2.2 Quantum Correction of Intensity   | <b>51</b>   |
| 4.2.3 Black Body Radiation Curve of Sun   | <b>55</b>   |
| 4.2.4 Solar Temperature   | <b>56</b>   |
| <b>Chapter 5 – DISCUSSION &amp; CONCLUSION</b>  | <b>57</b>   |
| <b>Appendix A – Intensity Distribution of Entire Solar Spectrum<br/>                  and star Sirius</b> | <b>63</b>   |
| <b>Appendix B – Line Spectra of Solar Elements</b>  | <b>82</b>   |
| <b>Line Spectra of Elements</b>   | <b>89</b>   |
| <b>Appendix C – Mechanism of producing line spectra of elements</b>                                       | <b>90</b>   |
| <b>List of Reference</b>  | <b>92</b>   |

## **DECLARATION**

“I certify that this dissertation does not incorporate without acknowledgement any material previously submitted for a Degree or Diploma in any University and to the best of my knowledge and belief it does not contain any material previously published or written or orally communicated by another person except where due Reference is made in the text.”

.....

Janaka Adassuriya

## **ACKNOWLEDGEMENTS**

I would like to make this opportunity to thank my project supervisor Dr. Chandana Jayaratne who has guided my efforts throughout the project. The knowledge and the precious advices that he gave me have been caused for effective completion.

I also thank Professor T. R. Ariyaratne, Head of the Department of Physics, for his encouragement to make the project a success.

Thanks are also due to the Arthur C. Clarke Institute of Modern Technology and its Director Mr. N. Kularatne for allowing me to use the telescope facilities at the ACCIMT.

I am especially grateful to research scientists Mr. Sarajh Gunasekara, Mr. Indika Medagangoda and Mr. Janthu Ferando of Arthur C. Clark Institute of Modern Technology, for their invaluable support through out the project. It is appreciable the knowledge that they share with me and the time they spent to make this project successful.

I have been fortunate to receive such a good support from my family and also my dearest friends who contributed in many ways.

# Introduction

---

There are infinite numbers of stellar objects in the universe. The electromagnetic radiation comes from them is the only way to investigate their characteristics. The spectrometric studies in the visible window had done a major contribution to seek the knowledge about the universe that we have today. Fortunately the spectra contain vast information about stellar objects and theories are developed to gain the accurate results.

The stars are so remote from the earth it may seem surprising that we can learn anything about their physical dimensions. We cannot perform experiments or alter conditions. So all we can do is to rely on observations. Stellar objects emit radiation in various ways. Especially stars emit energy in all range of wavelengths. The radiation is fallen throughout the electromagnetic spectrum. The only way to analyze the properties of stars is the light coming from them. The electromagnetic spectrum provides almost every information about stars.

The stars are selected according to the spectral types. Based on spectral types the stars are categorized in to seven major groups *viz.* O, B, A, F, G, K and M<sup>1</sup>. The spectra of these stars are almost identical. For particular spectral type, stars have their own characteristics, such as temperature, color index, and chemical composition. In the spectrum, the occurrence of a particular pattern of dark or bright lines characteristic to a certain element is evidence of the presence of that element. The dark lines in solar spectrum give evidence of the presence of certain chemical elements absorbing those wavelengths of the light between the sun and the earth.

This project is mainly focused on the analysis of solar spectrum. In addition, spectrum of the star Sirius too was obtained. A detail study of spectral lines of a star indicates its temperature, pressure, physical state of the gas in the star, magnetic and electric fields, whether the star is approaching or receding from us, etc. The main objective of this project is to develop a methodology to study the chemical composition and temperature of stars using the 45 cm GOTO reflective telescope located in the Arthur C. Clarke Institute of Modern Technology in Sri Lanka. This telescope is the biggest telescope in Sri Lanka which was commenced in 1996. All measurements were obtained using this telescope equipped with the spectrograph and a CCD camera.

Although the spectrometric study of stellar object is familiar to the world, in Sri Lanka we have no first hand experience. Astrophysics research conducting in this country is quite rare due to the limitations of resources and opportunities. As a preliminary step the project was focused around the developing of instrumental techniques for data collection and formulating the methodology of data analysis.

The computer software did the data analysis. The IRAF (Image Reduction and Analysis Facility) and CCDOPS are used here for data analysis. Due to the command – based function, IRAF is quite powerful and it is operating on LINUX operating system. The spectrums are basically analyzed by CCDOPS that is operating on windows and some applications of IRAF are also done.

## 1.1 Application of Spectroscopy

### 1.1.1 Discovery of expansion of the Universe

In 1912 V. M. Slipher<sup>5</sup> measured the radial velocities of galaxies by observing Doppler shift of their spectral lines and he found that all distant galaxies exhibit red shift, which indicates that they are receding from us. In 1929 E.Hubble<sup>5</sup> found that there exist a linear relationship between the velocities of recession of galaxies as measured by the red shift, and its distance from our own galaxy. Thus the further away a galaxy is, the faster it is receding. This is evidence of expanding universe.

The velocity of recession of a galaxy is given by Hubble's law<sup>5</sup>.

$$V = H_0 d \text{ ————— (1)}$$

V – Velocity of recession

d – Distance of galaxy

H<sub>0</sub> – Hubble's constant

The Figure 1.1 shows the red shift of several galaxies.

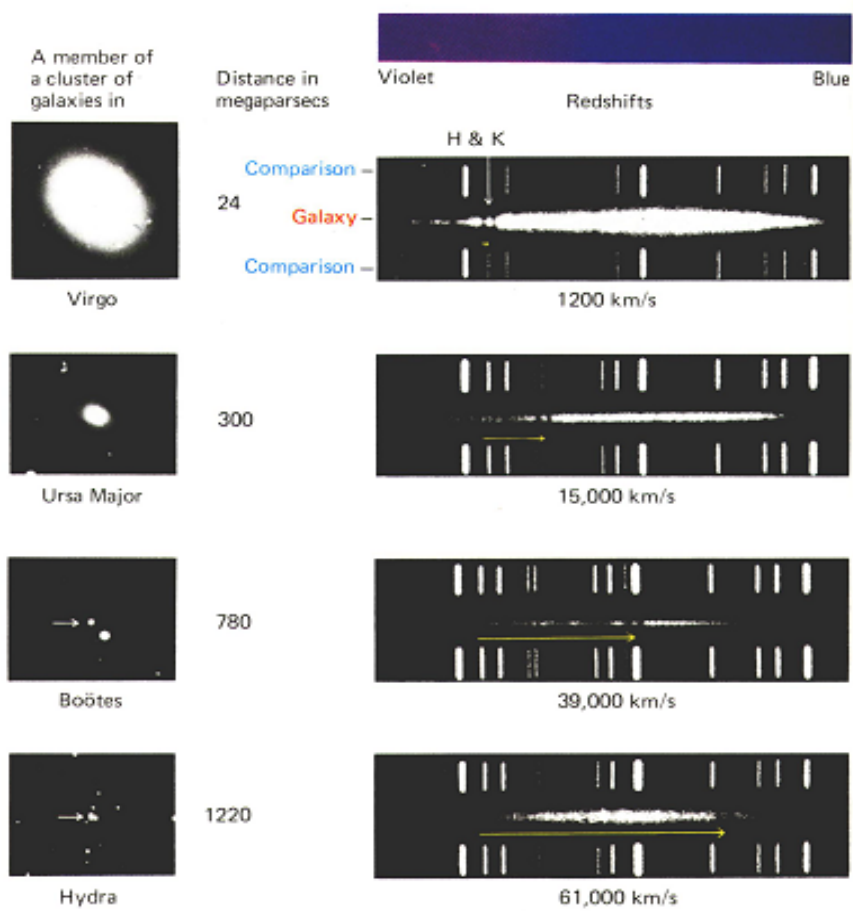


Figure 1.1 Red shift of the galaxies (Adapted from Pasachoff, 1991)

The spectra are shown at right corresponds the galaxies shown at the left, all produce at the same scale. Note that the apparent size of a galaxy reduces with increasing distance. The arrow below each horizontal streak of spectrum shows how far the H and K lines of ionized calcium are red shifted. The spectrum of emission line source located inside the telescope appears as vertical lines above and below each galactic spectrum to provide a comparison with a red shift known to be zero<sup>5</sup>.

### 1.1.2 Discovery of sodium in Mercury's thin atmosphere

In 1985 the sodium was discovered in Mercury with the ground-based telescope of the University of Texas, used for daytime observations of the planet at time when it was farthest from the sun<sup>5</sup>. The spectra of planetary surfaces show mainly the continuum and absorption lines of solar spectrum reflected to us. Surprisingly, spectra of Mercury showed not only the sodium absorption lines (the yellow D-lines) but also bright narrow emission lines. Some potassium has been discovered in a similar manner.

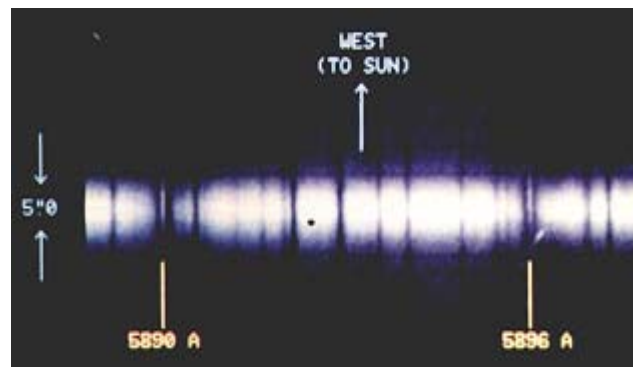


Figure 1.2 Sodium emission from planet Mercury.(Adapted from Pasachoff, 1991)

The figure 1.2 shows a photographic spectrum of planet Mercury - an enlargement of the smaller region of spectrum including the pair of sodium spectral lines known as the D lines. In general, Mercury's spectrum is similar to the sun. Since we observe reflected sun light; what we see is a continuous spectrum with several dark absorption lines. In the spectrum upon, each dark absorption line of sodium there is a bright emission line marked with the D-line wavelengths 5890 °A and 5896 °A, respectively. The emission lines show the presence of an atmosphere in the Mercury.

### 1.1.3 The use of the Doppler Effect to measure the period of rotation of the sun.

The period of rotation of the sun can be measured by taking a spectrogram of either the approaching or receding limb of the sun and comparing it with a spectrogram of the center of the sun made with the same equipment. This is achieved by aligning the slit of the spectroscope with whichever part of the sun it is desired to study. The approaching limb will show blue shifted spectral lines, and the lines of the receding limb will be red shifted. The figure illustrate how the spectroscope slit might be aligned at three successive positions over the sun's disc, and underneath diagrams show how the spectral line should be Doppler-shifted.

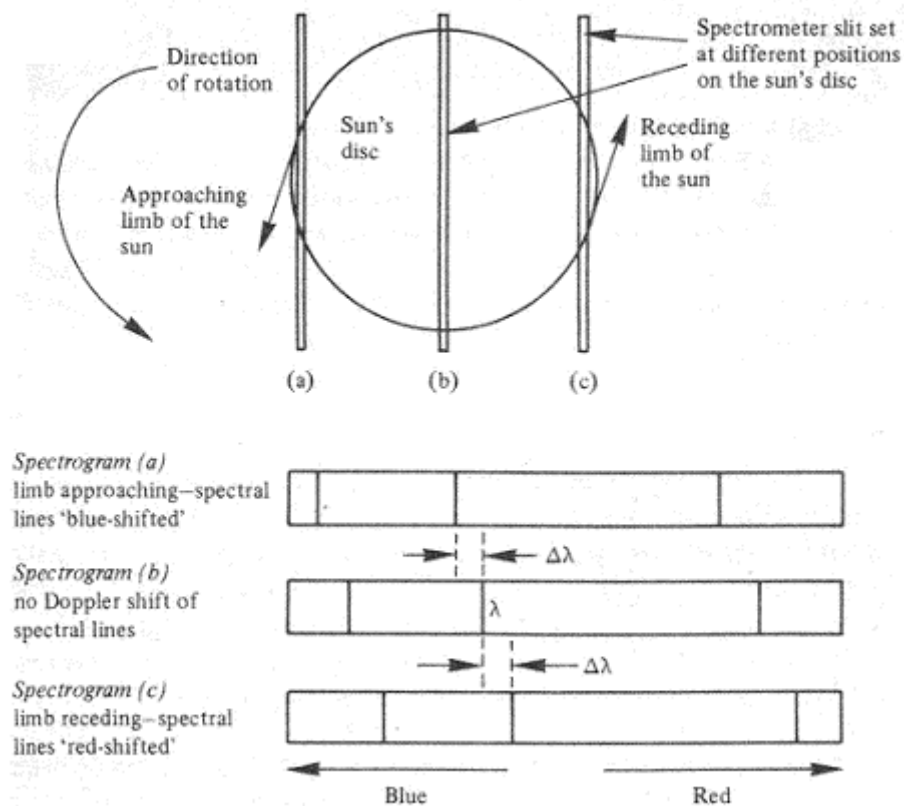


Figure 1.3 Red shift and blue shift of the rotating sun  
(Adapted from Donald, 1987)

The velocity of the limb towards or away from us is given by

$$\mathbf{V} = \mathbf{C} (\Delta\lambda / \lambda) \quad \text{—————} \quad (2)$$

Where **C** is the speed of light (  $3 \times 10^8 \text{ ms}^{-1}$  )

If the spectroscope was aligned, say the outer edge of the sun's disc and the radius of the sun is **r**, and then **V** represents that tangential velocity of the sun. The time period of the rotation is given by

$$\mathbf{T} = 2\pi\mathbf{r} / \mathbf{V} \quad \text{—————} \quad (3)$$

$$\mathbf{T} = 2\pi\mathbf{r} / (\mathbf{C} \Delta\lambda / \lambda) \quad \text{—————} \quad (4)$$

## ***Instrumentation***

---

The main instrumentations, which are needed for data collecting, are considered in this chapter. There are three instrumentations have been used for the experiment.

1. Charged Coupled Device (CCD) Camera
2. Spectrograph
3. Refractive Telescope

### **2.1 CCD camera**



Figure 2.1 ST-7 CCD camera

The CCD is very good at the most difficult astronomical imaging problem: imaging small, faint objects. The CCD based system has several advantages over film: greater speed, quantitative accuracy, ability to increase constant and subtract sky background with a few keystrokes, the ability to co-add multiple images without tedious dark room operations, wider spectral range, etc. These are ten times more sensitive than the fastest photographic films.

### 2.1.1 Function of CCD Camera

The highly sensitive silicon detectors amplify the tiny currents, which are generated by photons coming from faint objects. The light sensing area of the CCD is only 2.5 millimeters on a side, but it contains 32,680 light sensitive photo sites. Each photo sites consists of silicon substrata overlaid with an insulating layer of silicon dioxide and above that, etched strip of polysilicon. Each strip of polysilicon defines a line of photo sites. Within each line, the photo sites are separated by channel stops, thin strip of silicon that has Boron atoms implanted. The channel stops block the movement of electrons across columns within the silicon.

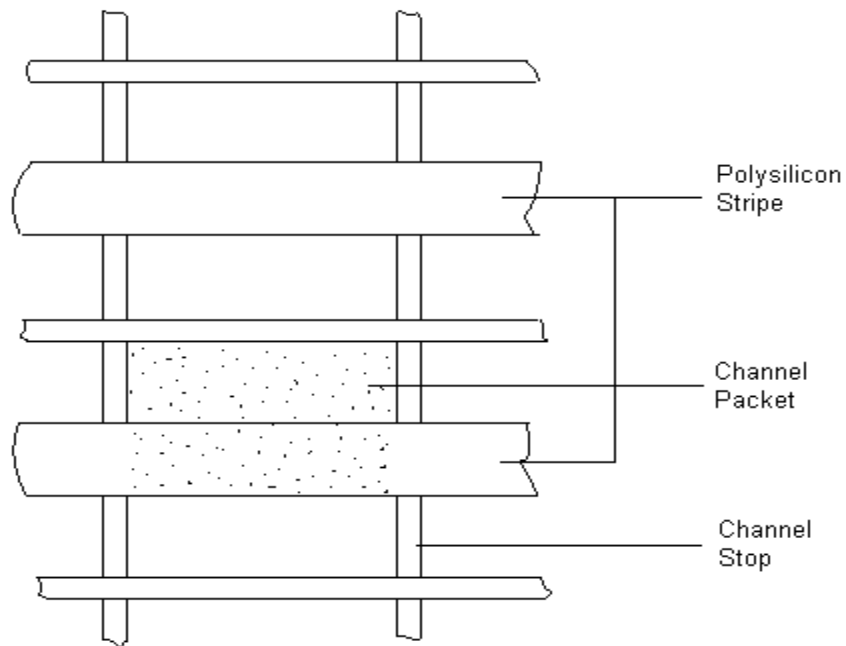


Figure 2.2 The structure of a silicon Cell of the CCD camera

When light falls on the CCD, photons pass through the polysilicon and silicon dioxide layer into the silicon. There they interact with atoms in the silicon crystal lattice, knocking electrons off the atoms according to the photoelectric effect.

The number of electrons knocked free is proportional to the number of oncoming photons. In a good CCD, as many as 60% of the incoming photons will knock out an electron. The electrons are trapped in potential wells, regions in the silicon layer where the electrical potential is highest. Each photo site is a potential well. During an exposure, incoming photons that accumulate in potential well, of the photo site.

In electronic terminology, the swarm of electrons becomes a “charge packet” trapped in a potential well.

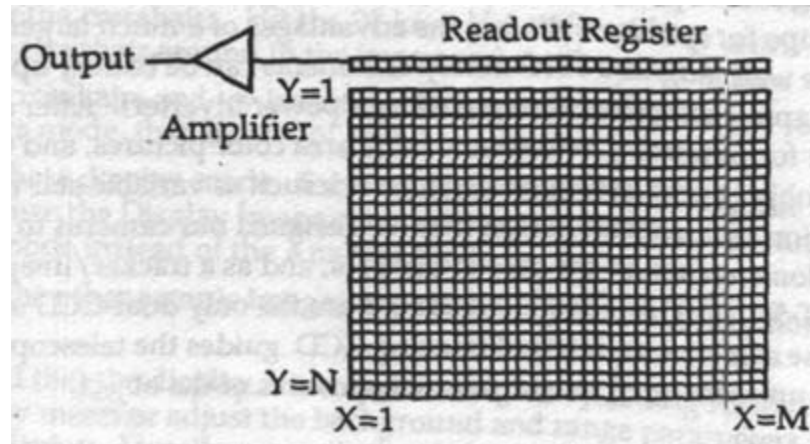


Figure 2.3 CCD array structure (Adapted from CCD operating manual)

To read out the chip, the serial register is cleared and the imaging area is cycled once delivering one line's worth of charge packets to the serial register. The serial register then transfers the line charge to the amplifier. Once again the image area is cycled and next line's worth of charge packets enters the serial register. This process is repeated until every charge packet of every line has been delivered to the amplifier.

The sensitive of any to adjacent photo site is probably the same within 1% and across the width of the chip there is no more than 10% variation. Each time a charge packet is transferred, 99.998% of electrons successfully shifted into the next potential well. Even after hundred of transfers, fewer than 1% of original electrons in a charge packet will be lost.

## 2.1.2 Camera Hardware Architecture

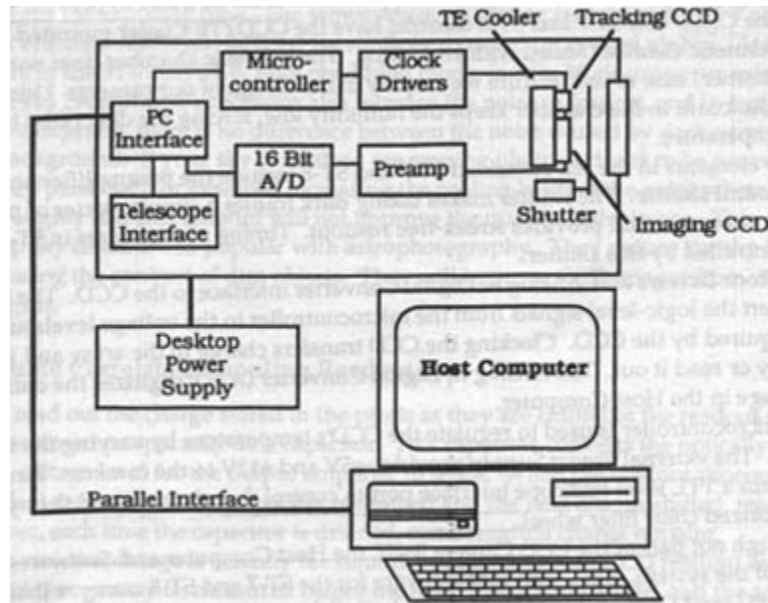


Figure 2.4 Hardware block diagram of CCD (Adapted from CCD operating manual)

The ST-7 camera is completely self-contained. The CCD is cooled by mounting it on the cold side of a thermoelectric (TE) cooler. The TE cooler pumps heat out of the CCD and dissipate it into a heat sink which forms part of the optical head's mechanical housing. Since the CCD is cooled below 0 °C, some provision must be made to prevent frost from forming on the CCD. The camera has the TE cooler mounted in a windowed hermetic chamber sealed with an O- Ring. The hermetic chamber does not need to be evacuated, because the rechargeable desiccant in the chamber keeps the humidity low, forcing the dew point below the cold stage temperature.

The shutter makes taking dark frames a simple matter of pushing a button on the computer and provides streak- free read out. Timing of exposure in ST-7 camera is controlled by this shutter. The Clock Driver and Analogue to Digital converter interface to the CCD. The clock drivers convert the logic level signals from the microcontroller to the voltage levels and sequence required by the CCD. Clocking the CCD transfers charge in the array and is used to clear the array or read it out. The A/D converter digitized the data in the CCD for storage in the host computer.

The microcontroller is used to regulate the CCD's temperature by varying the drive to the TE cooler. The external power supply provides  $\pm 5V$  and  $\pm 12V$  to the camera. The cameras contain a TTL level telescope interface port to control the telescope and the optional motorized color filter wheel.

### **2.1.3 CCD Cooling**

Random readout noise and noise due to dark current combine to place a lower limit on the ability of the CCD to detect faint light sources. All CCDs have dark current that can cause each pixel to fill with electrons in only a few seconds at room temperature even in the absence in the light. By cooling the CCD the dark current and the corresponding noise is reduced, and long exposures are possible. In fact, for roughly every  $5^\circ C$  of additional cooling, the dark current is reduced to half. At  $0^\circ C$  the dark current in the ST-7, high-resolution mode, is only 36 electrons per minute.

Although the CCD camera is a very sophisticated detecting device it has some limitations and statistics that define the performances of the camera. It is important to get an idea of these limitations for the optimum usage.

### 2.1.4 The Quantum Efficiency of CCD

The Quantum Efficiency is defining by the ratio of the number of photons detected by the camera to the number of photons incident on the camera. In other words the CCD's are not working with same efficiency in every wavelength. A particular camera works in particular wavelengths that its Quantum Efficiency is high. The CCD camera used here is ST-7 and its Quantum Efficiency is shown below.

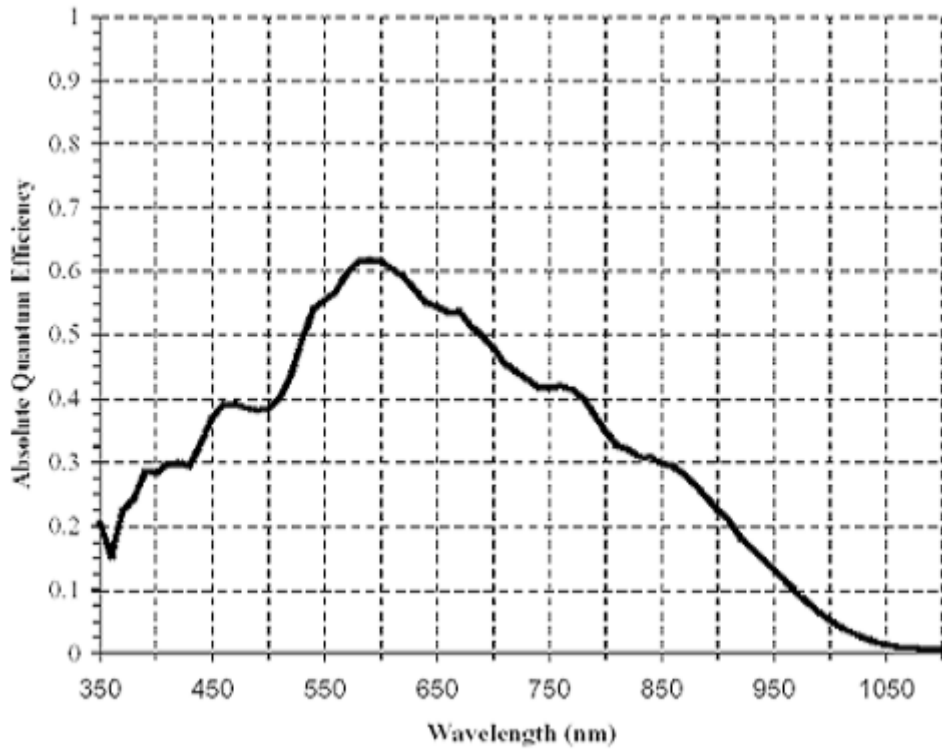


Figure 2.5 Quantum Efficiency of the ST – 7 CCD Camera  
( Adapted from SBIG web site)

### **2.1.5 Read - Out Noise**

Read - Out Noise is the irreducible “bottom line” for noises in the CCD chip, the random variation in the output of the CCD when no signal electrons are present. It is customarily expressed at the root mean square variation in number of electron detected by the CCD. Read - Out Noise is intrinsic to the CCD.

### **2.1.6 Linearity**

Ideally, the pixel value is directly proportional to the light that has fallen on the CCD. Therefore images from the camera can be precisely flat – field and used for precise astrometry and photometric measurements. As the charge wells on the CCD approach saturation, for example, the CCD become nonlinear; Charge skimming is a nonlinear response at low light levels. The goal of this test is to verify the linearity of the CCD over its full dynamic range or determine the range over which the CCD is linear so that the amplifier gain can be optimized.

### **2.1.7 Dark Current**

The accumulated charge from thermally generated electrons grows linearly with time. The noise due to the dark current is equal to the square root of the number of electrons accumulated during the integration time. Electrons are generated in the natural bulk silicon, in the charge depletion region, and in surface states at the interference between the bulk silicon and the silicon dioxide insulation layer. For this camera, the dark current is not significant until it accumulates to more than 280 electrons. Cooling the CCD reduced the rate at which thermal electrons are generated. Dark current can be reduced significantly by operating the CCD with the bias inverted, which reduced the contribution from surface states, but also reduce the full- well capacity.



Figure 2.6 Dark Frame of the ST-7 CCD Camera

Table 2.1 Specifications of the CCD camera used in this project

| Parameter          | Value                                |
|--------------------|--------------------------------------|
| CCD Camera Used    | KAF0400                              |
| Number of Pixels   | 765 x 510                            |
| Pixel Dimension    | 9 x 9 $\mu$                          |
| Array Dimension    | 6.9 x 4.6mm                          |
| Read Noise         | 15e <sup>-</sup> rms                 |
| Full Well Capacity | 40Ke <sup>-</sup> /80Ke <sup>-</sup> |

## 2.2 Spectrograph

The spectrograph is an apparatus with which the spectrum of a light source can be photographed or otherwise recorded. Attached to a telescope, the spectrograph can be used to record the spectrum of the light from a particular star. Light from the source enters from the spectrograph through a narrow slit and it then collimated (made into beam of parallel rays) by a lens. The collimating light is entering a grating, causes different wavelengths of light leave in different directions, because of dispersion. The second lens placed behind the grating forms an image an image of the spectrum on the CCD camera.

The grating dispersed light of different wavelengths enters the second lens from slightly different directions, and consequently the lens produce a different of the slit for each different wavelength. The multiplicity of different slit images of different colors lined up at the photographic emulsion is the desired spectrum.

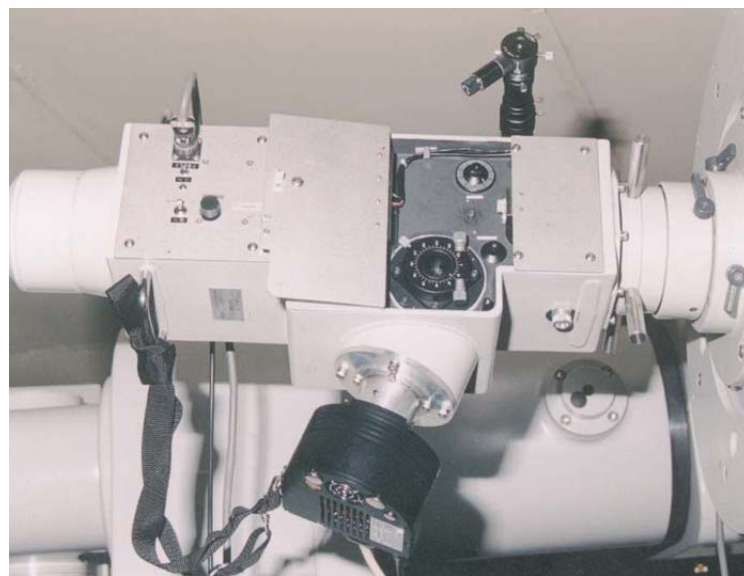
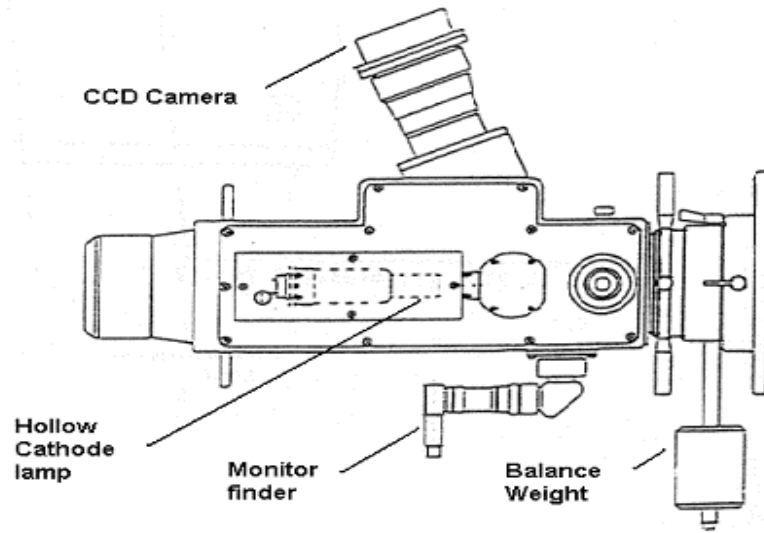


Figure 2.7 the spectrograph used for the measurement

Table 2.2 Specification of the spectrograph.

|                          |          |   |
|--------------------------|----------|---|
| Range of Wavelength      |          | 3600 – 7000 °A  |
| Dispersion               |          | Approximately 90 °A/mm  |
| Collimator               |          | Off axis parabolic mirror f = 385 mm  |
| Slit                     |          | Length : 3 mm (maximum)<br>Width : 0 – 10 mm  |
| Dispersion System        |          | Grating : Reflection Type Plane Diffraction<br>Grating<br>Grooves : 900 line/mm<br>Blaze Wavelength : 5500 A<br>Ruled Area : 64x64 mm |
| Comparative Light Source |          | Hollow Cathode Lamp (steel)   |
| Wide Field Finder        | Eyepiece | f : 26 mm Illuminated Reticle   |
|                          | Field    | 13  |
| Monitor Finder           | Eyepiece | f : 6 mm Illuminated Reticle  |
|                          | Field    | Approximately 5mm diameter on the slit  |
| Filter                   |          | L-38 In addition to that, it is possible to mount 2 pieces of standard size 50x50 mm  |
| Outside Dimension        |          | Total Length : approximately 760 mm<br>Weight : 26 kg   |

## ***Experimental Procedure***

---

### **3.1 Observation of Line Spectra**

The Spectral Photography is very sensitive and cautiously recorded because the spectrum is the only data that is coming from the unknown stellar objects. Although there are advanced facilities (Automatic Telescope, CCD Camera) the observer's skill is very vital to get the superior results.

Initially the full range of Solar Spectrums was obtained using the following procedure. The normal sunlight was adequate to take the spectrum. It does not need to move the telescope to the direction of the sun. But the distant stars must be clearly focused with the slit. The computer operated Telescope has the capability to track a star. First the characteristics of a star such as spectral class, magnitudes are found using the sky software package. Then according to these parameters the star number is finding from a data book. Such data book contains around 15000 stars. The number was given to the Telescope operating software and Telescope will then finding the star itself. The Monitor Finder of the Spectrograph provides the view, to focus the star on the slit.

If the star is not symmetrically situated on the slit the hand set of the Telescope is used for slight adjustments. When the star is focused on the slit it is ready to get the image. The Hollow Cathode Lamp current is adjusted to a sufficient value. The full spectrum is observed by changing the grating angle.

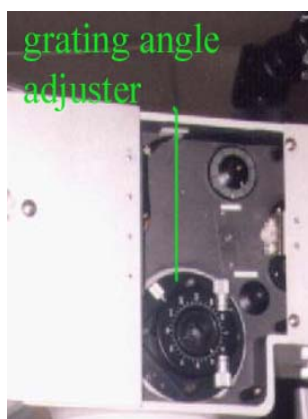


Figure 3.1 Adjustable knob of the grating angle.

The spectral image was detected by using the CCD camera. Before download the spectral images the CCD temperature was set to a low temperature usually  $-7^{\circ}\text{C}$  to  $-3^{\circ}\text{C}$ . The low temperature reduces Dark Current which is mentioned in the previous chapter. The CCD was focused by using the CCDOPS software. The exposure time was manually selected frame by frame according to the image type and light conditions. At the end of spectral image downloading the Dark Frame must be taken in order to make the dark current correction..

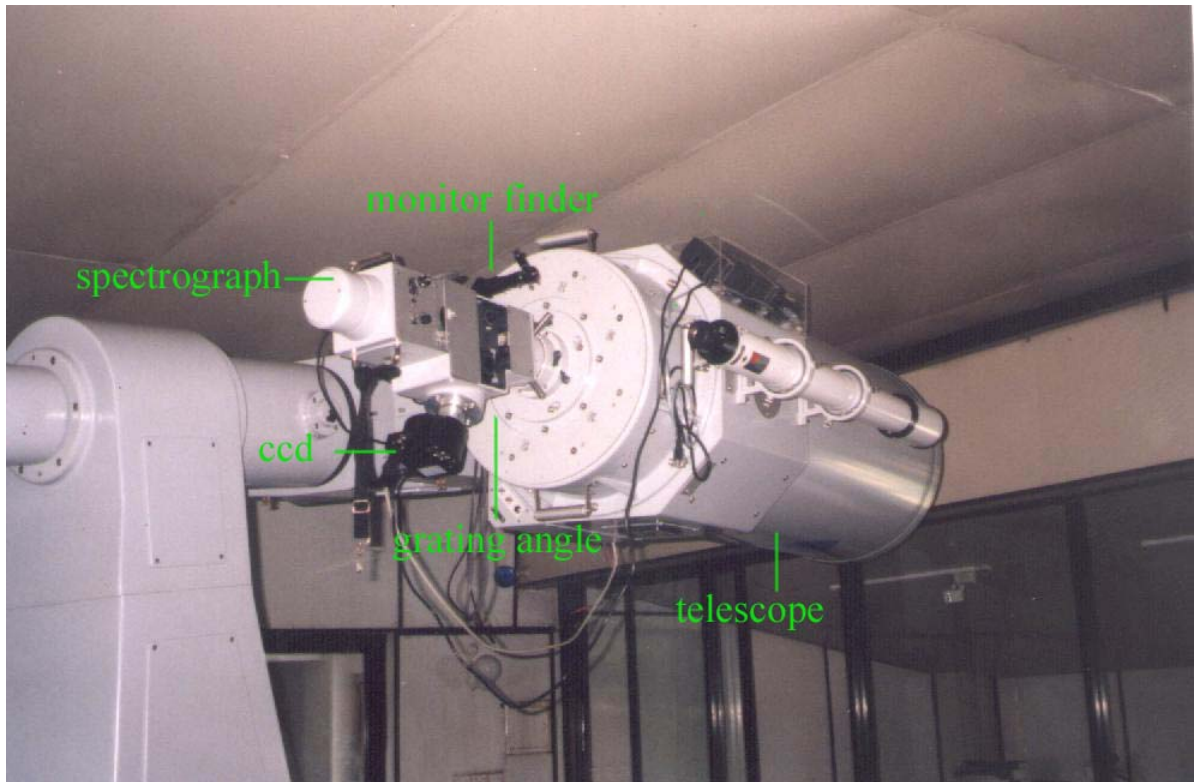


Figure 3.2 The complete apparatus used for stellar objects observations.

**4.1 Identification of Chemical Composition of the Solar Spectrum**

This chapter is focused on the analysis of absorption spectrum of the sun. The dark lines are prominent in the absorption spectrum. These dark lines indicate missing wavelengths due to the absorption of radiation. Each particular chemical element or compound, when in the gaseous form, produces its own characteristic pattern of dark or bright lines. In other words, each particular gas can absorb or emit only certain wavelengths of light, characteristic to that gas. The presence of a particular pattern of dark lines characteristic of a certain element or chemical compound is evidence of the presence of that element or compound somewhere along the path of the light whose spectrum has been analyzed.

**4.1.1 Line Identification**

The line identification will be done by the wavelength calibration. The arc spectrum is very important in this calibration procedure. A reference arc spectrum is produced by the Hollow Cathode which is located inside the spectrograph. Every spectrum consists of reference emission lines with different intensities. The figures 4.1 and 4.2 show a spectrum with hollow cathode reference lines.

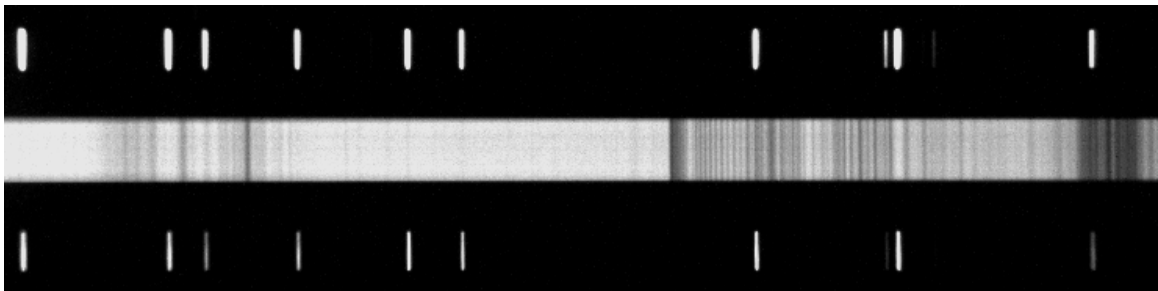


Figure.4.1 Normal Solar Spectrum

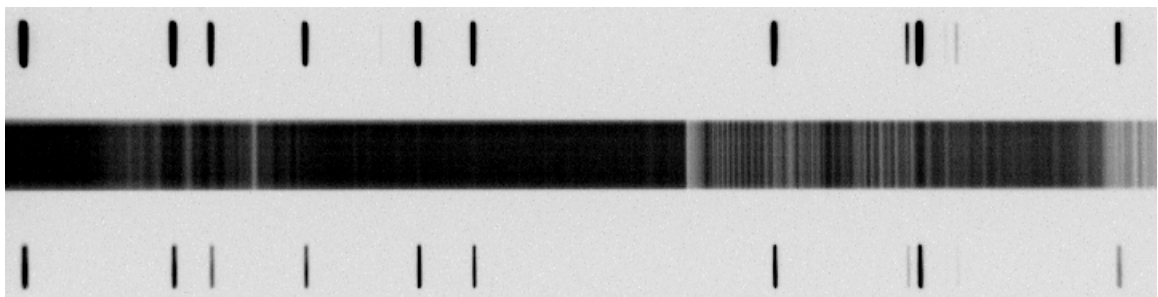


Figure.4.2 Inverted Solar Spectrum

### **4.1.2 Reference Lines Matching**

Initially the reference lines must be identified. In order to identify reference lines, emission line wavelengths of hollow cathode are provided as an image. The intensity vs wavelength is plotted over the wavelength range of 3000 Å-10000 Å in these images. The arc lines are identified by considering the intensity and the distance of two arc lines, and match with the plotted hollow cathode images. If the spectral reference lines are matched with intensity lines of the image, those lines can be identified by the wavelengths mentioned in the intensity lines. The figure 4.3 shows the matched reference lines with intensity image of hollow cathode.

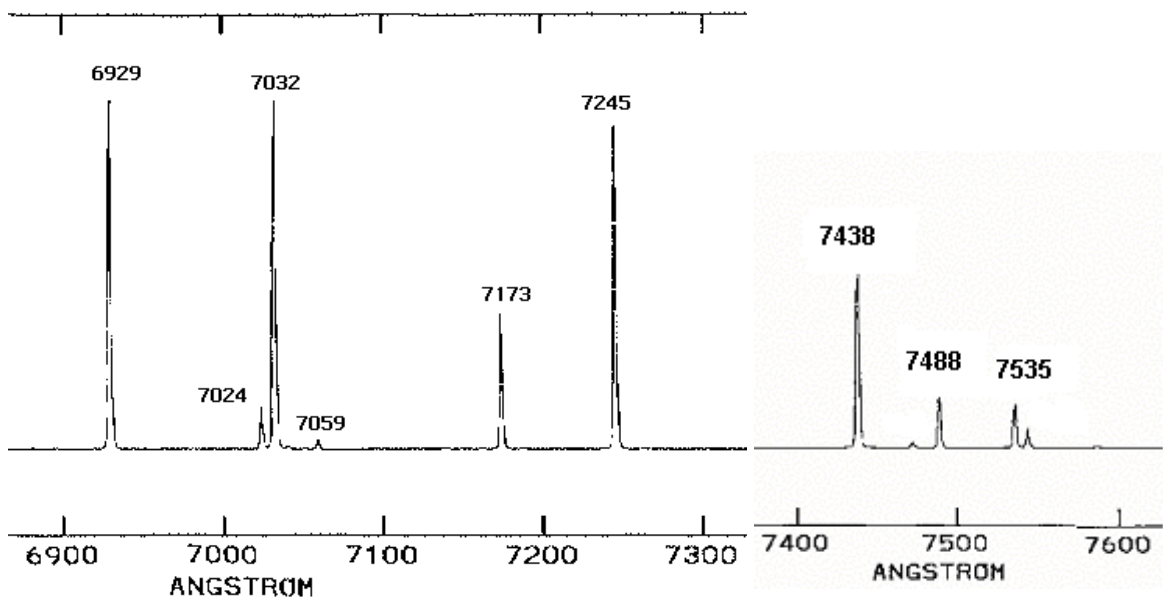
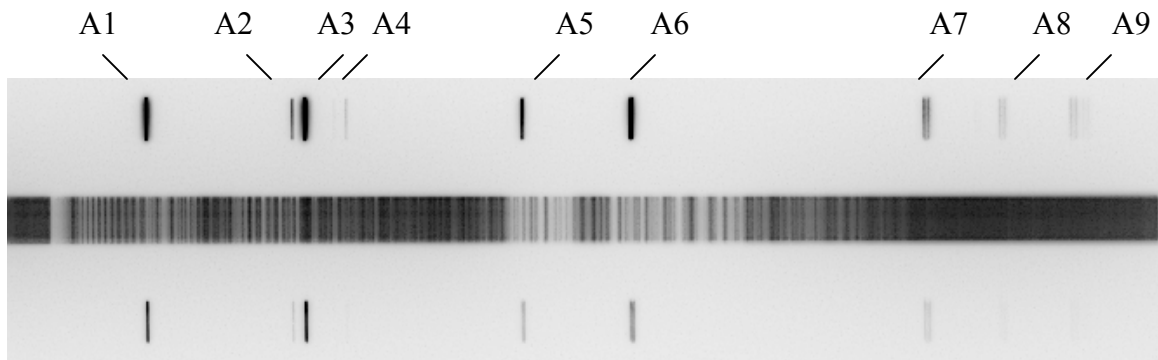
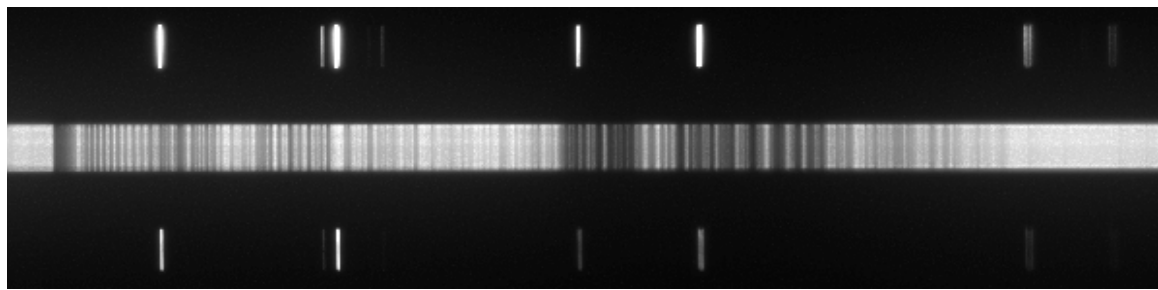


Figure 4.3 The reference emission lines A1...A9 of hollow cathode are matched with the intensity lines of hollow cathode spectrum.

The lines A1, A2, A3, A4, A5, A6, A7, A8, A9 are matched with wavelengths and tabulated in the table 4.1.

Table 4.1 The Wavelengths of Reference Lines of Solar Spectrum obtained using the Figure 4.3

| Spectral Line | Wavelength $\lambda$ ( $\text{\AA}$ ) |
|---------------|---------------------------------------|
| A1            | 6929                                  |
| A2            | 7024                                  |
| A3            | 7032                                  |
| A4            | 7059                                  |
| A5            | 7173                                  |
| A6            | 7245                                  |
| A7            | 7438                                  |
| A8            | 7400                                  |
| A9            | 7535                                  |

#### 4.1.3 The identification of pixel points of reference lines

It is necessary to find out the pixel value of emission lines of hollow cathode with the higher accuracy. The CCDOPS (CCD Software) provide the facility to identify the pixel position anywhere in the spectral image. The X and Y coordinate and the intensity of particular point can be read out by the software. The wavelength of arc lines change in X direction only. Therefore the X value of the pixel point is sufficient for the wavelength calibration.

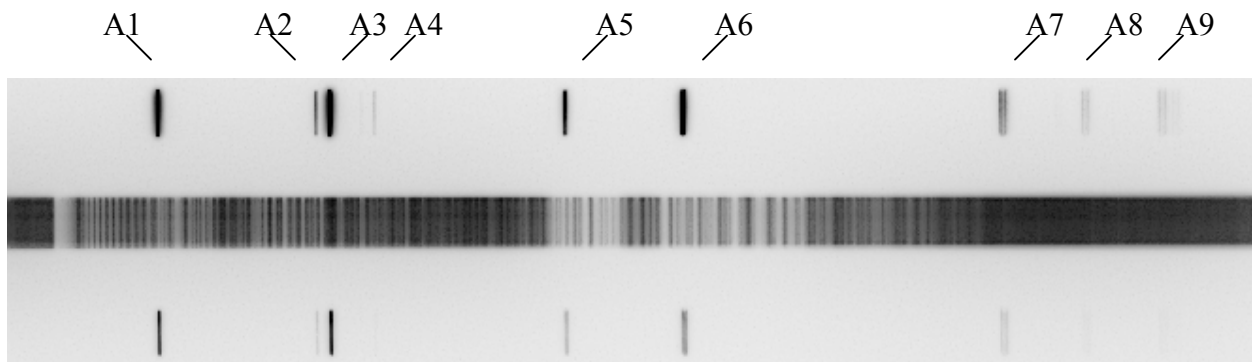


Figure. 4.4 The pixel point identification of the solar spectrum

The line wavelengths of A1...A9 and the corresponding X value of pixel points are tabulated in the table 4.2.

Table 4.2 The Pixel Points of the Reference Lines are obtained using Figure 4.4

| Spectral Line | Wavelength $\lambda$ (A) | Pixel Point |
|---------------|--------------------------|-------------|
| A1            | 6929                     | 81          |
| A2            | 7024                     | 164         |
| A3            | 7032                     | 172         |
| A4            | 7059                     | 195         |
| A5            | 7173                     | 296         |
| A6            | 7245                     | 360         |
| A7            | 7438                     | 529         |
| A8            | 7488                     | 573         |
| A9            | 7535                     | 614         |

The wavelength is proportional to the X value of pixel point since the pixel points and wavelengths are linearly distributed.

$$\text{Wavelength } (\lambda) \propto \text{Pixel Point } (X) \quad \text{—————} \quad (5)$$

The graph of wavelength ( $\lambda$ ) vs pixel point (X) is found to be a straight line. The graph was plotted and a typical plot is shown in the figure 4.5.

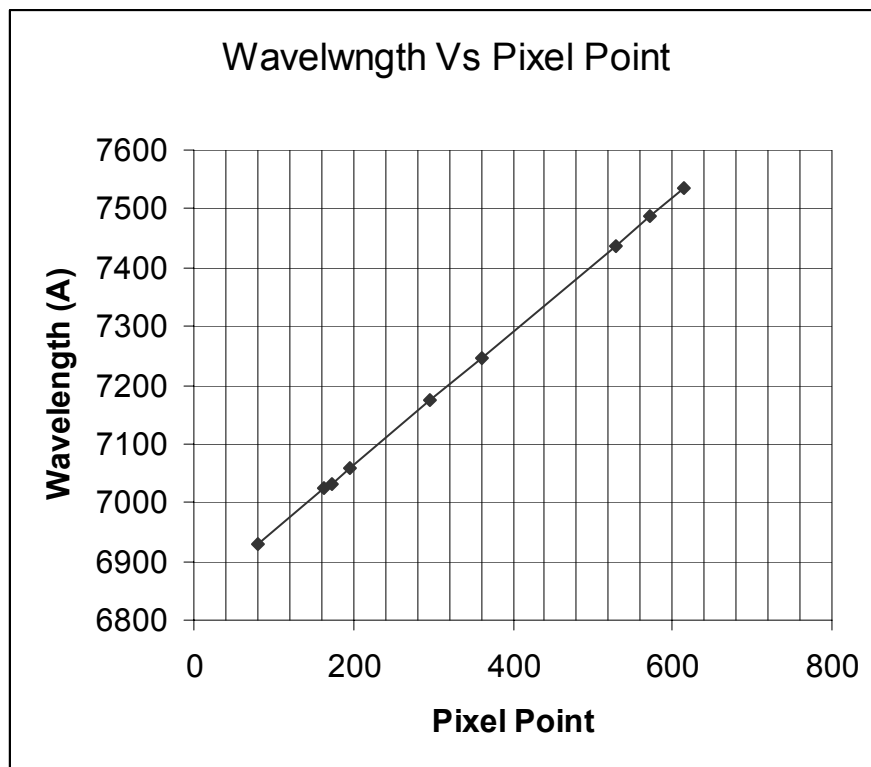


Figure 4.5 Graph of wavelength vs pixel point of the reference lines

The graph is the wavelength calibration for line identification. If the pixel point is known for particular absorption line of spectrum, the wavelength can be calculated by the equation of straight line.

To achieve grate accuracy the gradient (m) and interceptor (c) must be obtained carefully. Although the Excel has the facility to calculate the line equation it may be deviated from precise value, as the graph is plotted on the graph paper to minimize the errors.

The above procedure was followed to analyze the Solar Spectrum. The visible part of the Solar Spectrum (4000 A – 7000 A) was obtained by changing the grating angle of the spectrograph.

#### 4.1.4 Solar Spectrum (7200 – 7600)°A

The Solar Spectrum obtained at the Grating Angle 37° of the Spectrograph.

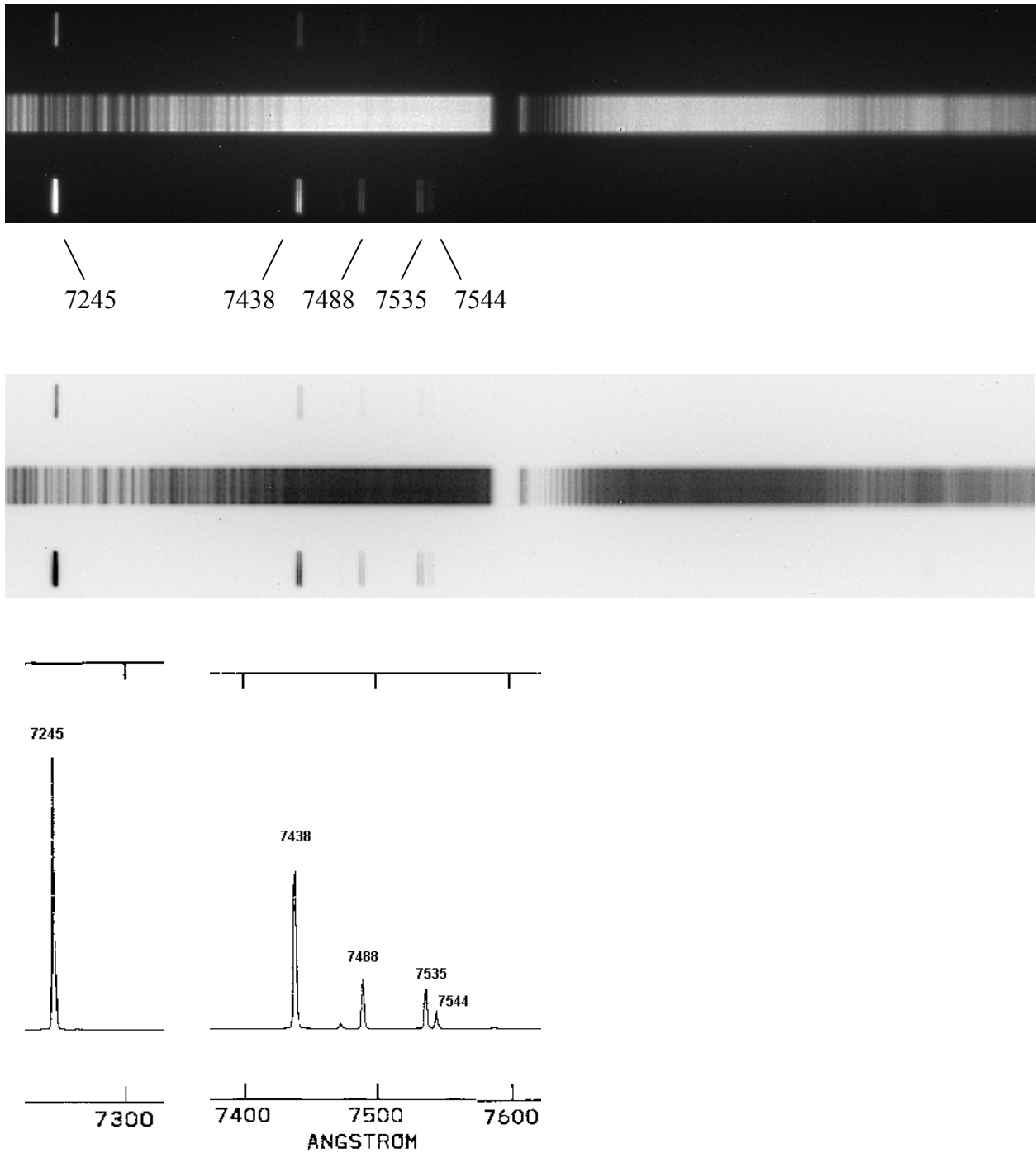


Figure.4.6 The reference line identification of range 7200 – 7700 °A of the solar spectrum with the intensity spectrum of the hollow cathode.

The pixel points corresponding to the above reference lines are identified by CCDOPS and shows in the table 4.3.

Table 4.3 Pixel Points of Reference Lines (for 7200-7700 °A range)

| Wavelength $\lambda$ (°A) | Pixel Point |
|---------------------------|-------------|
| 7245                      | 36          |
| 7438                      | 206         |
| 7488                      | 250         |
| 7535                      | 291         |
| 7544                      | 298         |

The Graph of wavelength vs pixel point is shown in the figure 4.7.

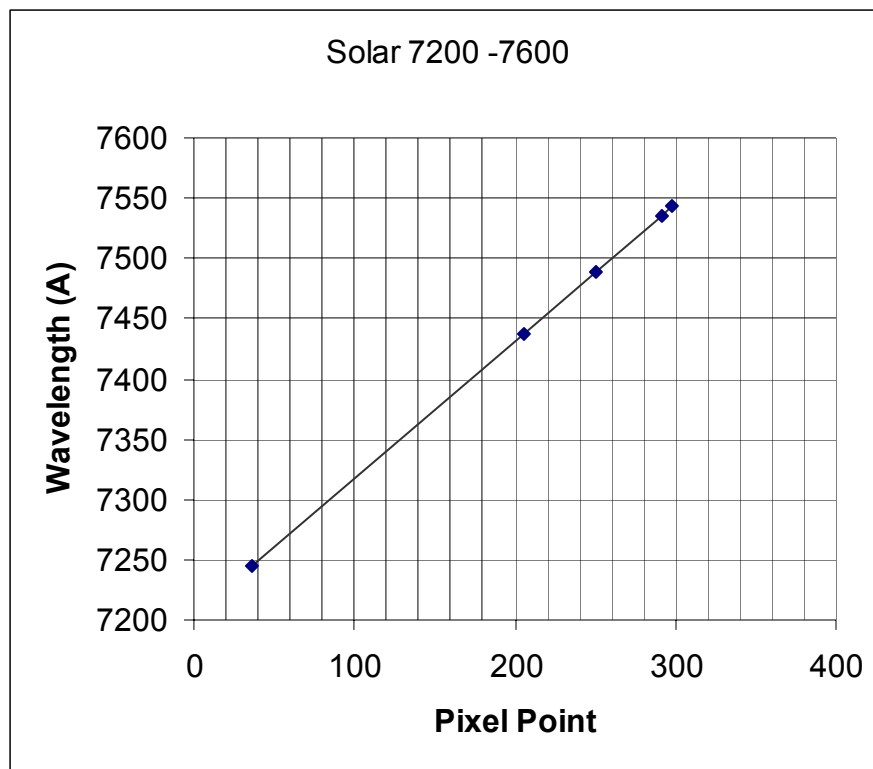


Figure 4.7 Graph of wavelength of reference lines vs pixel points (for 7200 – 7700 °A range)

$$\text{Gradient (m)} = 1.1636$$

$$\text{Intercept (c)} = 7198$$

Equation of straight line

$$Y = 1.1638 X + 7198 \text{ ——— (4.1)}$$

The pixel points (x) of prominent absorption lines of the solar spectrum shows in the figure 4.6, are identified and the corresponding wavelengths are calculated according to the equation (1). The wavelengths are matched with line spectra wavelengths of elements and radicals to identify what element or radical is responsible for create absorption lines in the spectrum. The line spectra of elements are found out from the Chemistry & Physics Hand Book<sup>6</sup> and through the Internet. The line spectra wavelengths are attached to the appendix. The obtained results are presented in table 4.4

Table 4.4 The Identified Absorption (dark) Lines of Solar Spectrum (for 7200 – 7700 °A range) and Corresponding Elements or Molecules.

| Pixel Point (x) | Wavelength (°A) | Elements/Molecules                           |
|-----------------|-----------------|--|
| 11              | 7210.80         | } Hydrocarbon<br>} Radicals &<br>} Molecules |
| 26              | 7228.25         |  |
| 36              | 7239.89         |  |
| 42              | 7246.87         |  |
| 64              | 7272.47         |  |
| 77              | 7286.43         |  |
| 87              | 7299.23         |  |
| 93              | 7306.21         |  |
| 100             | 7314.36         |  |
| 114             | 7330.65         |  |
| 127             | 7345.77         |  |
| 156             | 7380.68         |  |
| 164             | 7388.83         |  |

The identified wavelengths belong to molecules especially Hydrocarbon radicals. Also the atmospheric absorption bands are occurred and Fig. 4.8 shows one of them. The scale of wavelength is also provided for the convenience.

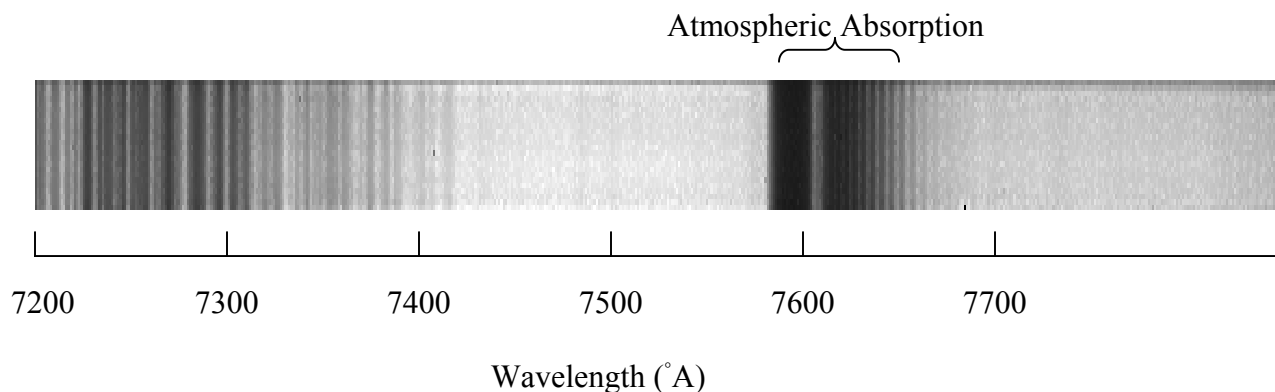


Figure 4.8 Absorption lines of elements of solar spectrum ( 7200-7700 °A range)

### 4.1.5 Solar Spectrum (6800 – 7300) Å

The Solar Spectrum obtained at the Grating Angle 39° of the Spectrograph.

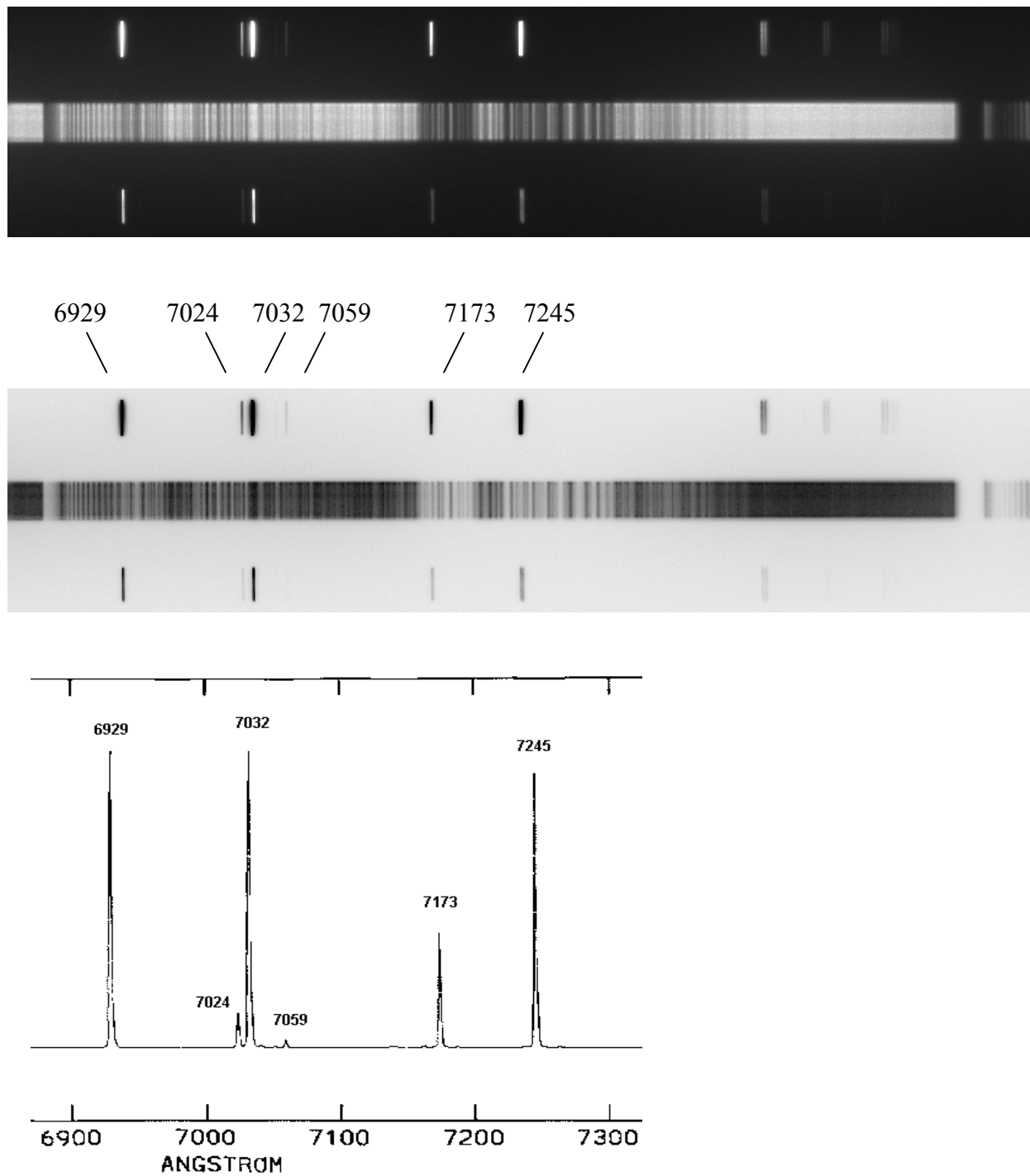


Figure. 4.9 The reference line identification of range 6800 – 7300 Å of the solar spectrum with the intensity spectrum of the hollow cathode.

The pixel points corresponding to the above reference lines are identified by CCDOPS and shows in the table4.5.

Table 4.5 Pixel Points of Reference Lines (for 6800-7300 °A range)

| Wavelength (°A) | Pixel Point |
|-----------------|-------------|
| 6929            | 81          |
| 7024            | 164         |
| 7032            | 172         |
| 7059            | 195         |
| 7173            | 296         |
| 7245            | 360         |

The Graph of Wavelength vs Pixel point is shown in the figure.

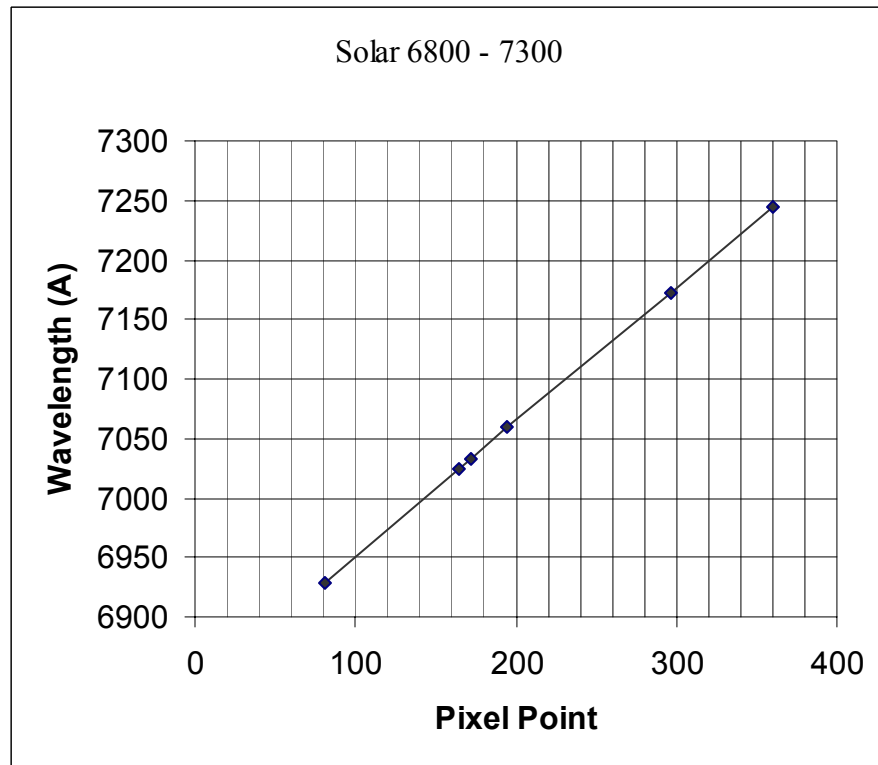


Figure 4.10 Graph of wavelength of reference lines vs pixel points (for 6800-7300 °A range)

Gradient (m) = 1.1607

Interceptor (c) = 6833

Equation of the line

$$Y = 1.1607 X + 6833 \quad \text{———— (4.2)}$$

The prominent absorption lines of solar spectrum in figure are identified and calculate the corresponding wavelengths using equation (4.2). Hence matched the wavelengths and find out the elements of the absorption lines. The results are tabulated in table 4.6

Table. 4.6 Identified Absorption Lines of the Spectrum (for 6800 – 7300 °A range) and Corresponding Identified Elements or Molecules.

| Pixel Point | Wavelength (°A) | Element/Molecules | Intensity of line |
|-------------|-----------------|-------------------|-------------------|
| 350         | 7239.24         |                   | 1263 p            |
| 335         | 7221.83         |                   | 2376 p            |
| 308         | 7190.49         |                   | 1171 p            |
| 296         | 7176.57         |                   |                   |
| 257         | 7091.16         |                   | 3756              |
| 213         | 7080.23         |                   | 3500 p            |
| 189         | 7052.37         |                   | 3279 p            |
| 177         | 7038.44         |                   | 3171 p            |
| 168         | 7027.99         |                   | 3172 p            |
| 158         | 7016.39         | Si                | 2675 p            |
| 148         | 7004.78         | Si                | 2429 p            |
| 91          | 6938.62         |                   | 2390 p            |
| 82          | 6928.17         | Ne                | 2511 p            |
| 76          | 6921.21         |                   | 2738 p            |

p – indicate prominent absorption lines

The identified lines are marked in the spectrum.

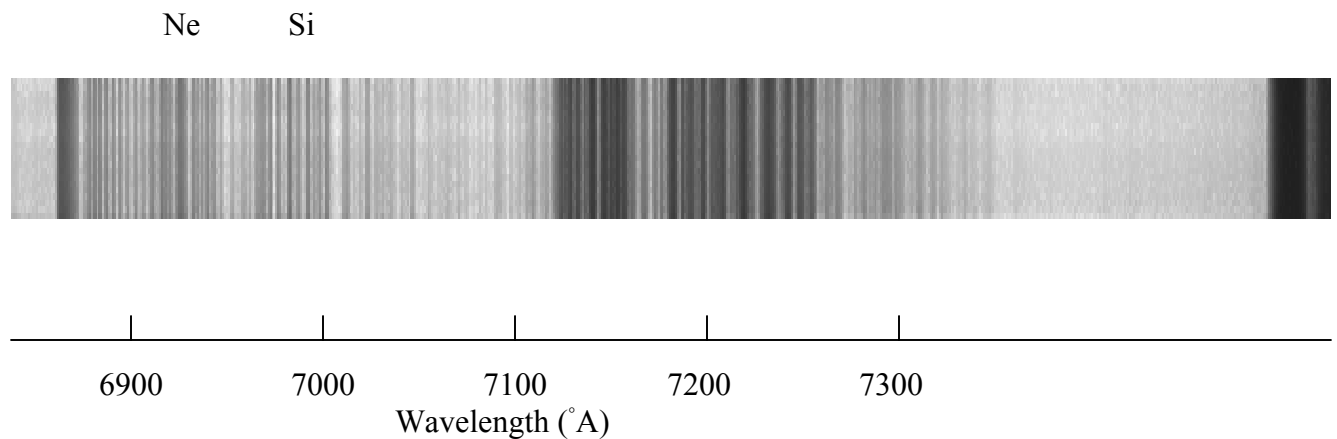


Figure 4.11 Absorption lines of elements (for 6800-7300 °A range)

#### 4.1.6 Solar Spectrum (6200 – 6900) °A

The Solar spectrum obtained at the Grating Angle 41° of the Spectrograph.

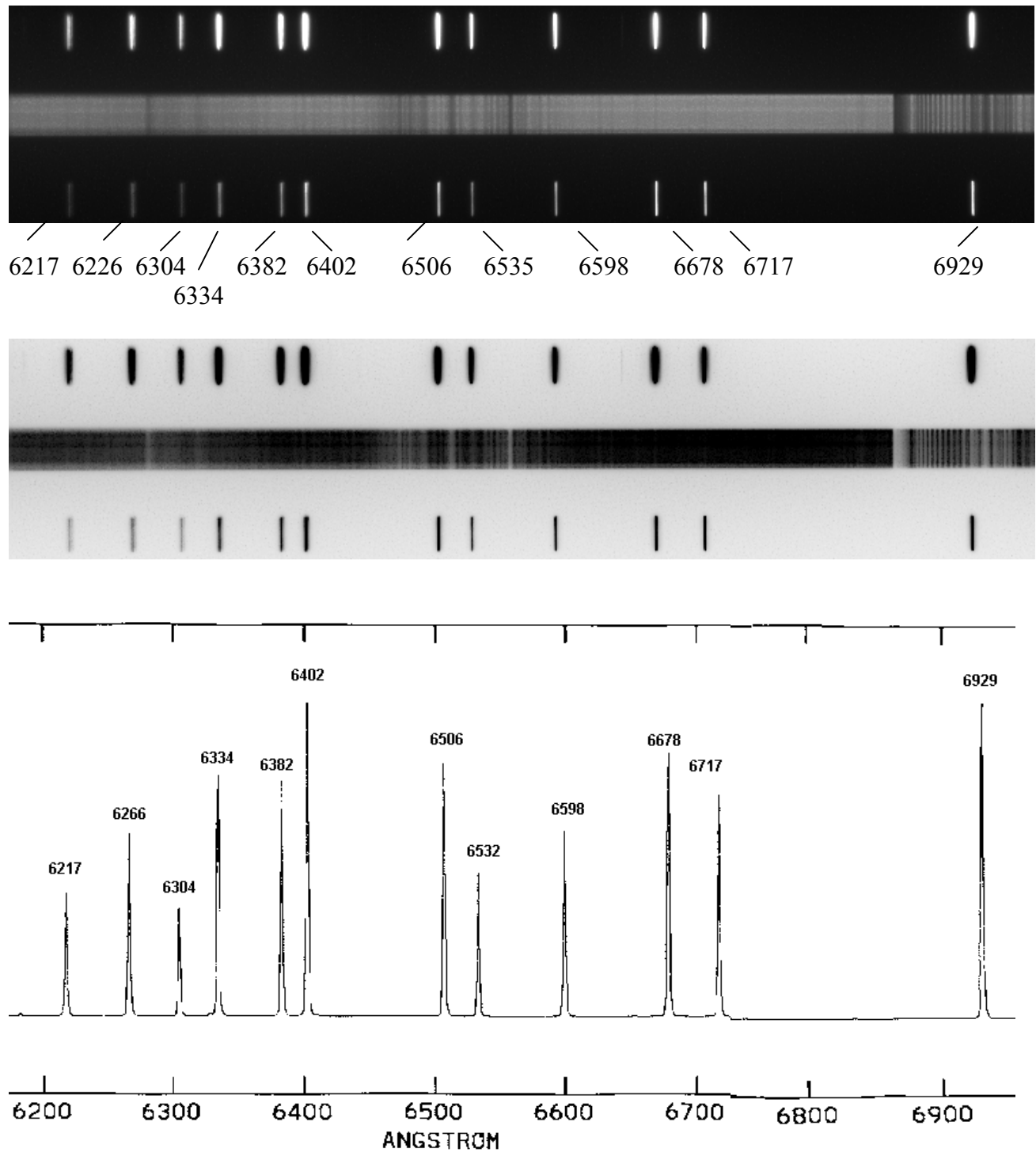


Figure 4.12 Reference lines identification of range (6200-6900 °A)

The corresponding pixel points, for the reference lines of solar spectrum of the figure, are listed in the table.

Table 4.7 Pixel Points of Reference Lines (for 6200-6900 °A range)

| Wavelength (°A) | Pixel Point |
|-----------------|-------------|
| 6217            | 43          |
| 6304            | 122         |
| 6334            | 149         |
| 6382            | 192         |
| 6402            | 210         |
| 6506            | 303         |
| 6532            | 326         |
| 6598            | 385         |
| 6678            | 455         |
| 6717            | 490         |

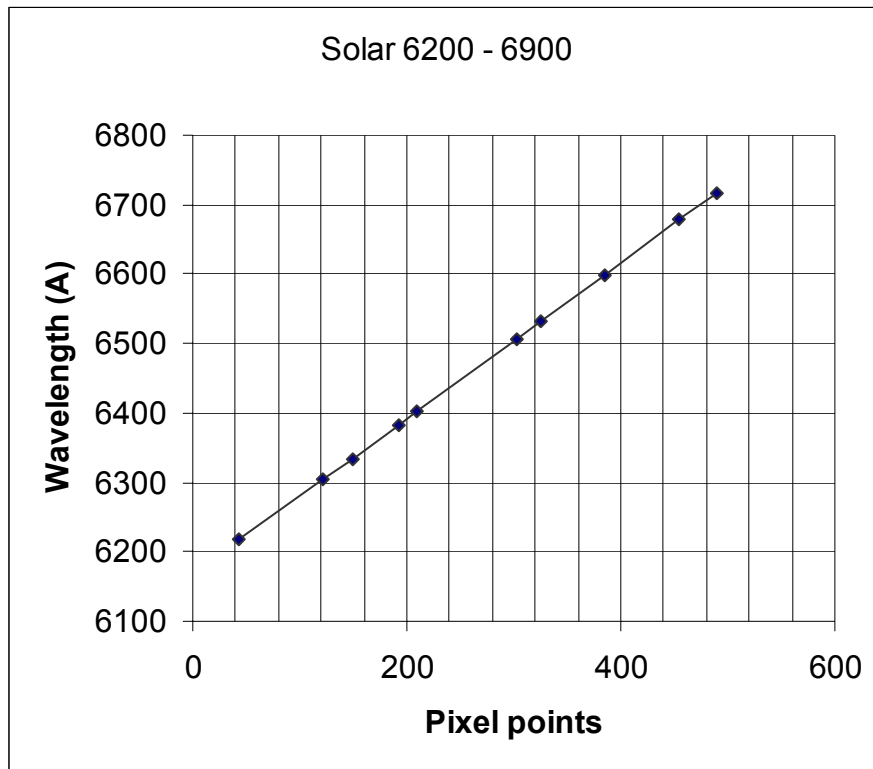


Figure 4.13 Graph of wavelength of reference lines vs pixel points (for 6200-6900 °A range)

Gradient(m) = 1.1294

Interceptor(c) = 6165

Equation of straight line

$$Y = 1.1294 X + 6165 \text{ ————— (4.3)}$$

The wavelengths of identified absorption lines are tabulated in the table.

Table 4.8 Identified Absorption Lines of Spectrum (for 6200-6900 °A range) and Corresponding Elements.

| Pixel Point | Wavelength (°A) | Element    | Intensity |
|-------------|-----------------|------------|-----------|
| 99          | 6276.80         |            | 1593 p    |
| 275         | 6475.58         | Bi         | 1696 p    |
| 282         | 6483.49         | Ba         | 1696 p    |
| 292         | 6494.78         | Fe         | 1908 p    |
| 312         | 6517.00         | Cu         | 1618 p    |
| 353         | 6563.00         | H $\alpha$ | 1365 p    |
| 374         | 6587.00         | C          | 2037      |
| 380         | 6594.00         |            | 2130      |
| 455         | 6679.00         | He         | 2310      |

p- indicates the prominent lines

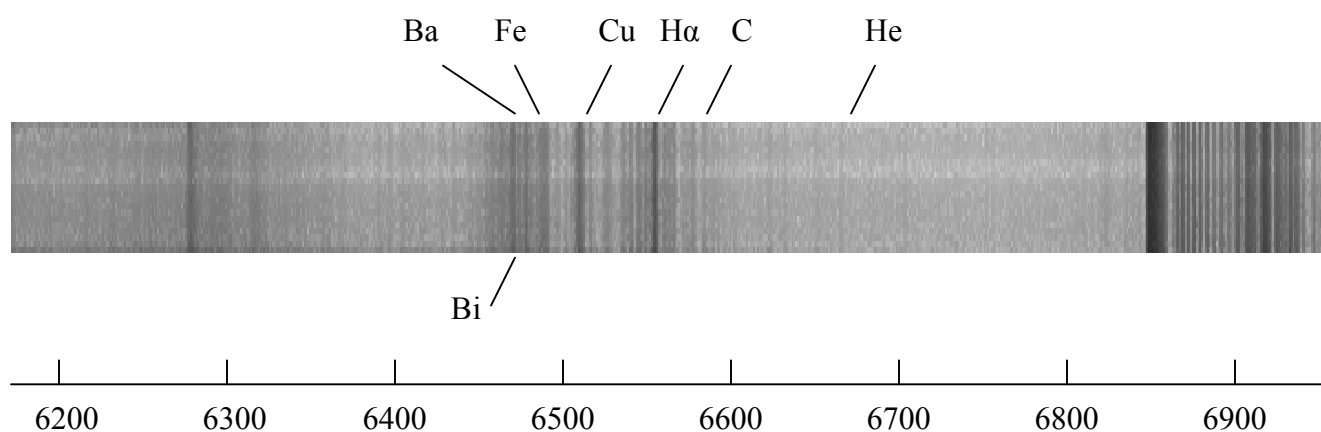


Figure 4.14 Absorption lines of elements (6200-6900 °A range)

### 4.1.7 Solar Spectrum (5900 – 6200) °A

The Solar spectrum obtained at the Grating Angle 42° of the Spectrograph.

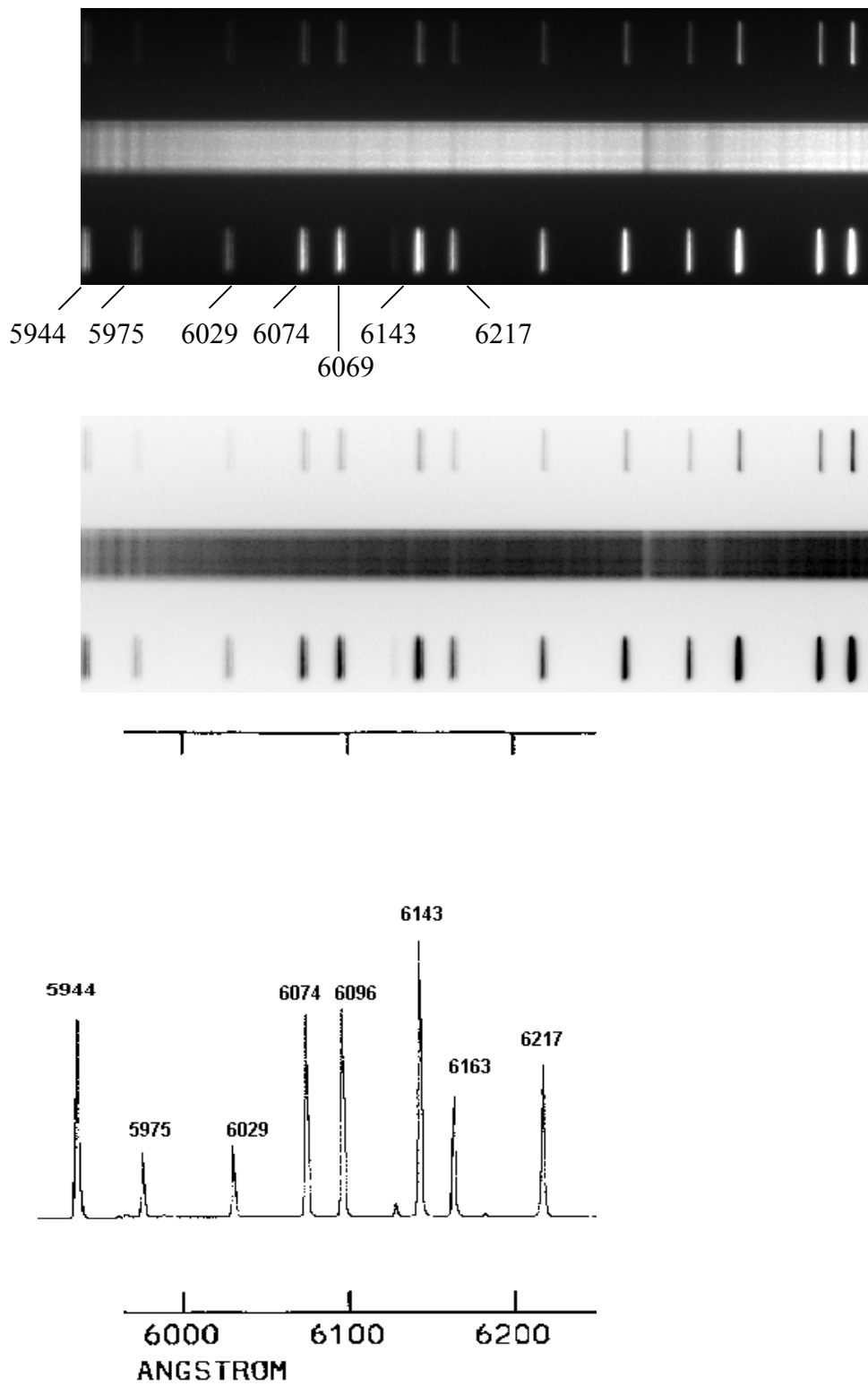


Figure 4.15 Reference line identification of range ( 5900-6200 °A range)

The corresponding pixel points for the reference lines are in the table.

Table 4.9 Pixel Points of Reference Lines (5900-6200 °A range)

| Wavelength (°A) | Pixel Point |
|-----------------|-------------|
| 5944            | 3           |
| 5975            | 30          |
| 6029            | 80          |
| 6074            | 120         |
| 6096            | 140         |
| 9143            | 182         |
| 6163            | 200         |
| 6217            | 248         |

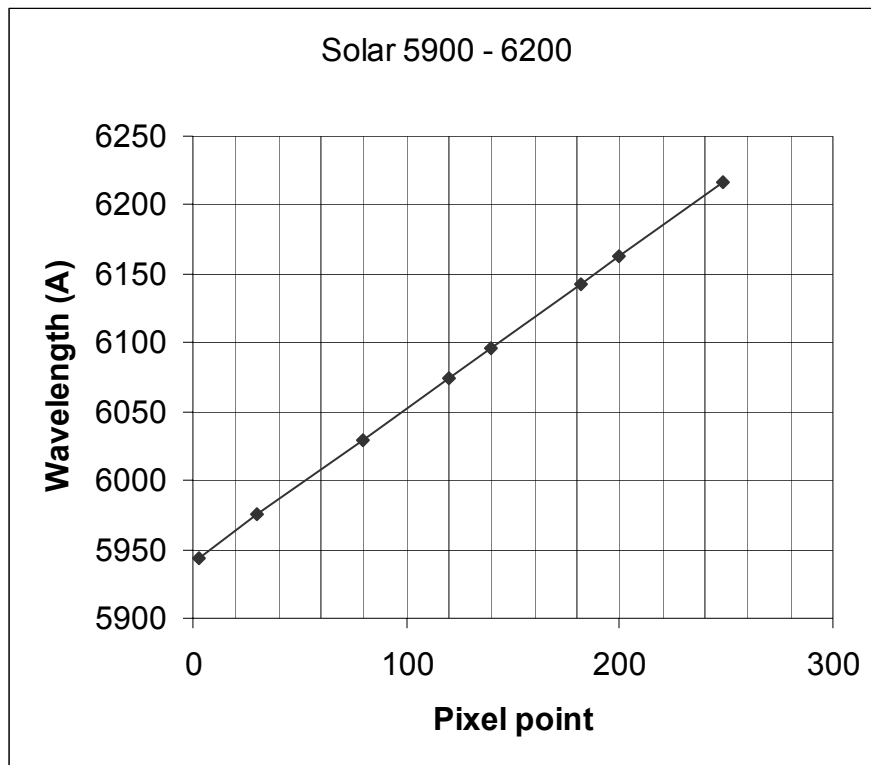


Figure 4.16 Graph of wavelength of reference lines vs pixel points (5900-6200 °A range)

Gradient (m) = 1.1

Interceptor (c) = 5943

Equation of the Straight Line

$$Y = 1.1 X + 5943 \quad (4.4)$$

The wavelengths of absorption lines are calculated using equation (4) and results are tabulated in the table.

Table 4.10 Identified Absorption Lines of Spectrum ( 5900-6200 °A range) and Corresponding Elements

| Pixel Point | Wavelength (°A) | Identified Element | Intensity of the line |
|-------------|-----------------|--------------------|-----------------------|
| 17          | 5961.50         | Fe                 | 3409                  |
| 25          | 5970.30         |                    | 3232 p                |
| 34          | 5980.20         |                    | 3394 p                |
| 147         | 6105.60         |                    | 4504                  |
| 178         | 6138.60         | Fe                 | 4608                  |
| 200         | 6162.80         |                    |                       |
| 304         | 6277.00         |                    | 3791                  |

p – Indicates the prominent lines

The identified absorption lines are shown in the figure.

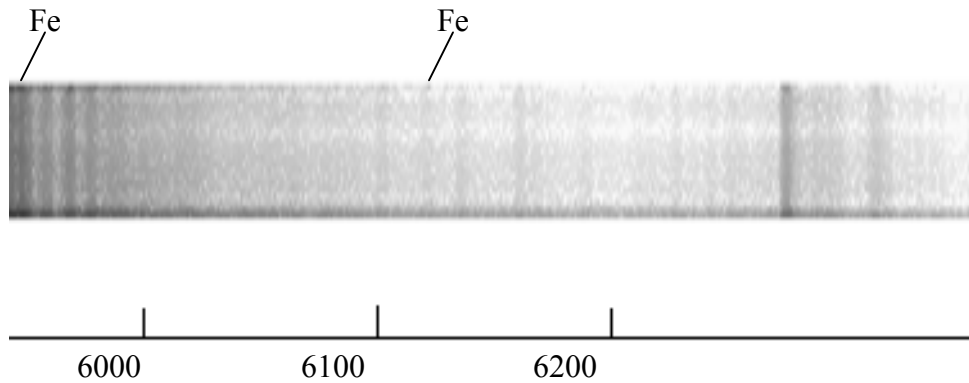


Figure 4.17 Absorption lines of elements ( 5900-6200 °A range)

### 4.1.9 Solar Spectrum (4200 – 5000) °A

The Solar spectrum at Grating Angle 49° of the Spectrograph

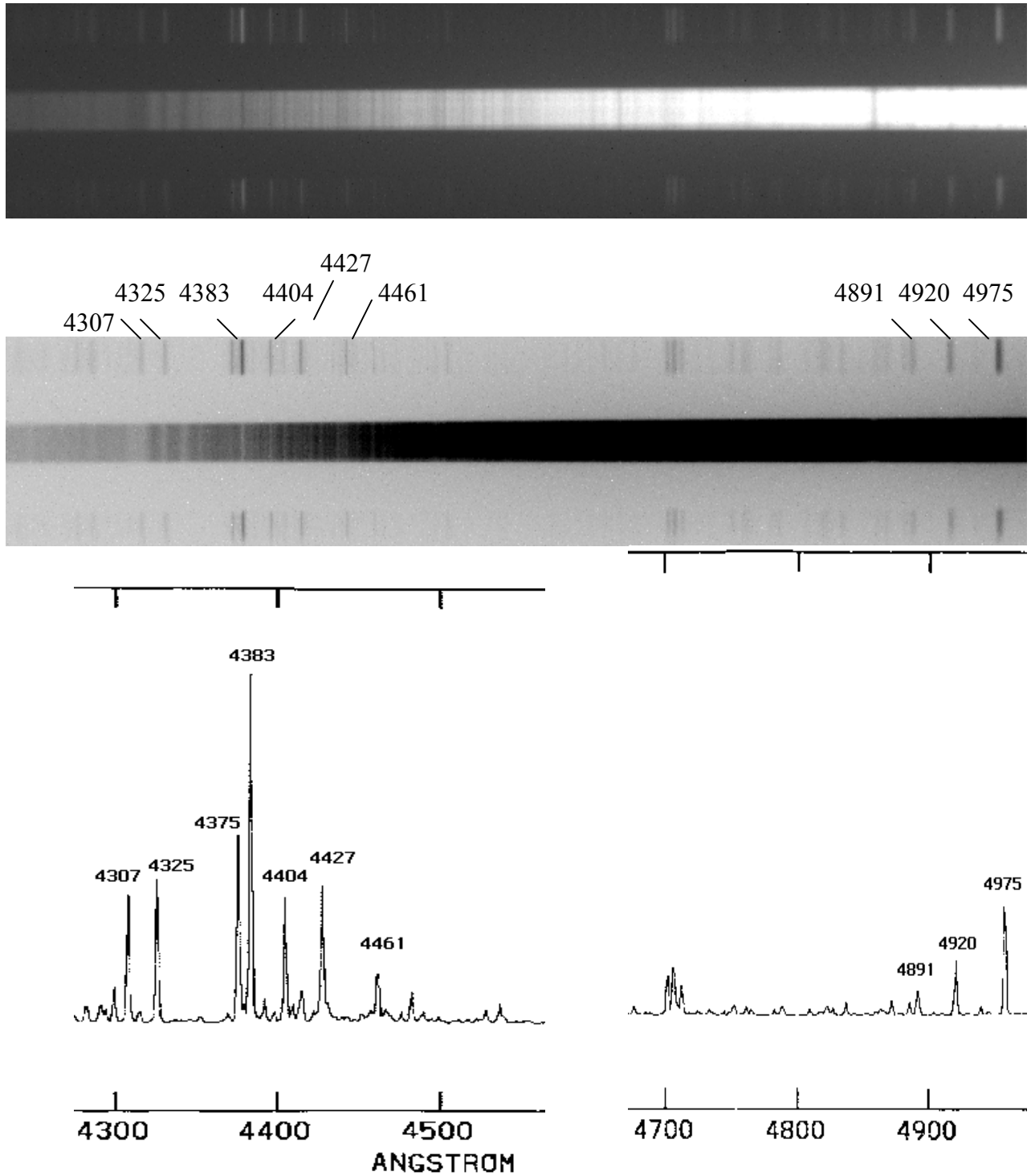


Figure 4.21 Reference line identification of range ( 4200-5000 °A range)

The corresponding pixel points for the reference lines are shown below.

Table 4.13 Pixel Points of Reference Lines ( 4200-5000 °A range)

| Wavelength (°A) | Pixel Point |
|-----------------|-------------|
| 4307            | 96          |
| 4325            | 113         |
| 4375            | 160         |
| 4383            | 168         |
| 4404            | 187         |
| 4427            | 209         |
| 4461            | 241         |
| 4891            | 640         |
| 4920            | 666         |
| 4957            | 701         |

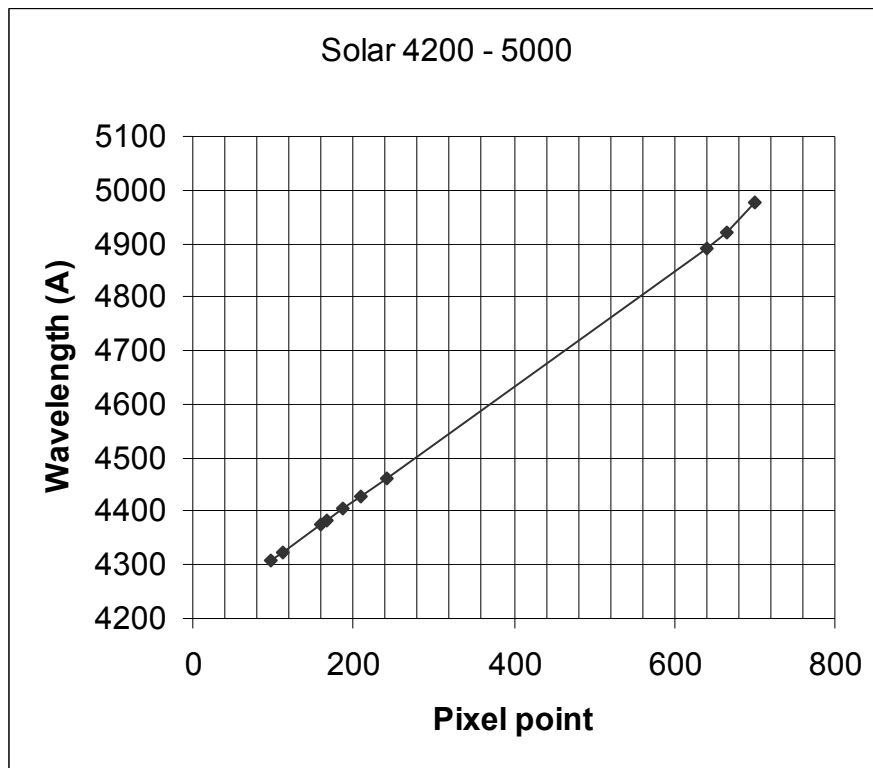


Figure 4.22 Graph of wavelength of reference lines vs pixel points ( 4200-5000 °A range)

Gradient (m) = 1.075

Interceptor (c) = 4203

Equation of the straight line

$$Y = 1.075 X + 4203 \quad (4.6)$$

The wavelengths of absorption lines are calculated using the equation (4.5) and find out the corresponding element responsible for the absorption lines. The table shows the results.

Table 4.14 Identified Absorption Lines of Spectrum (4200-5000 °A range) and Corresponding Elements

| Pixel Point | Wavelength (°A) | Identified Elements | Intensity of the line |
|-------------|-----------------|---------------------|-----------------------|
| 112         | 4323.40         | Fe                  | 261 p                 |
| 126         | 4338.45         | H $\gamma$          | 258 p                 |
| 168         | 4383.60         | Fe                  |                       |
| 187         | 4404.00         | Fe                  |                       |
| 198         | 4415.85         | Fe                  | 442 p                 |
| 223         | 4442.72         |                     |                       |
| 260         | 4482.50         | Fe                  | 526 p                 |
| 310         | 4536.25         | Mg                  | 605 p                 |
| 434         | 4669.55         | Na                  | 740 p                 |
| 490         | 4729.75         | Mg                  | 932 p                 |
| 613         | 4862.00         | H $\beta$           | 873 p                 |
| 640         | 4891.00         | Fe                  | 1070                  |
| 667         | 4920.00         | Fe                  | 1075                  |
| 702         | 4957.65         | Fe                  | 1207                  |
| 726         | 4983.45         |                     | 1143                  |

P – Indicates, Prominent Lines.

The identified lines are marked in the figure.

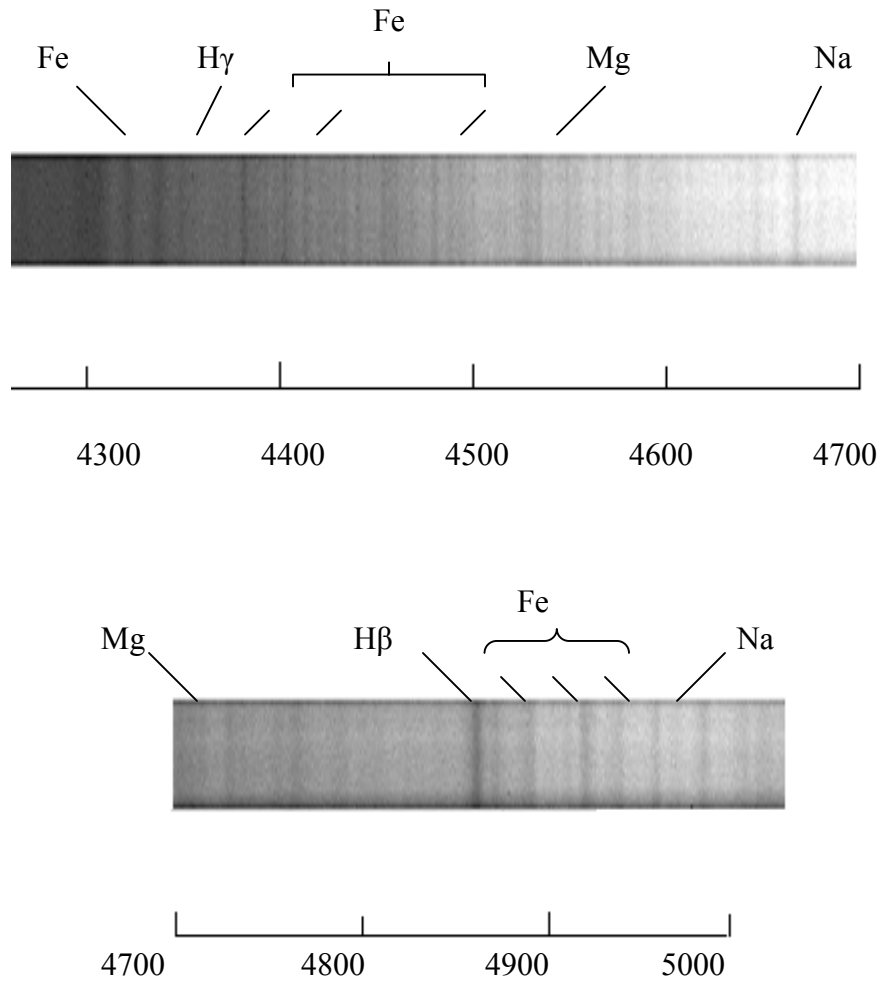


Figure 4.23 Absorption lines of elements ( 4200-5000 °A range)

#### 4.1.10 Solar Spectrum (4100 – 4400) °A

The Solar spectrum obtained at Grating Angle 50° of the Spectrograph.

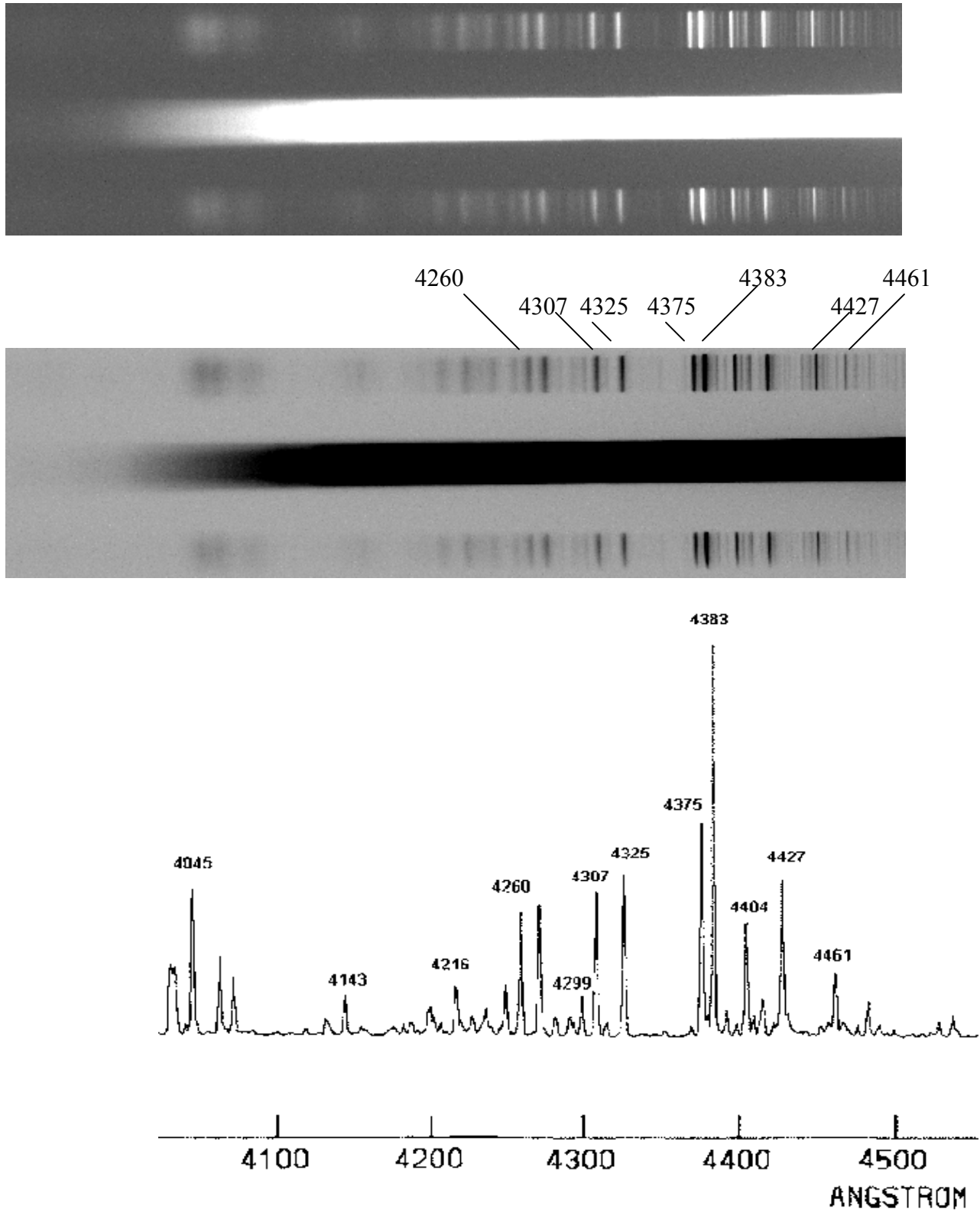


Figure 4.24 Reference line identification of range (4100-4400 °A)

Table 4.15 Pixel Points of Reference Lines (4100 – 4400 °A range)

| Wavelength (°A) | Pixel Point |
|-----------------|-------------|
| 4216            | 478         |
| 4260            | 519         |
| 4299            | 556         |
| 4307            | 563         |
| 4325            | 580         |
| 4375            | 627         |
| 4383            | 634         |
| 4404            | 654         |
| 4427            | 675         |
| 4461            | 707         |

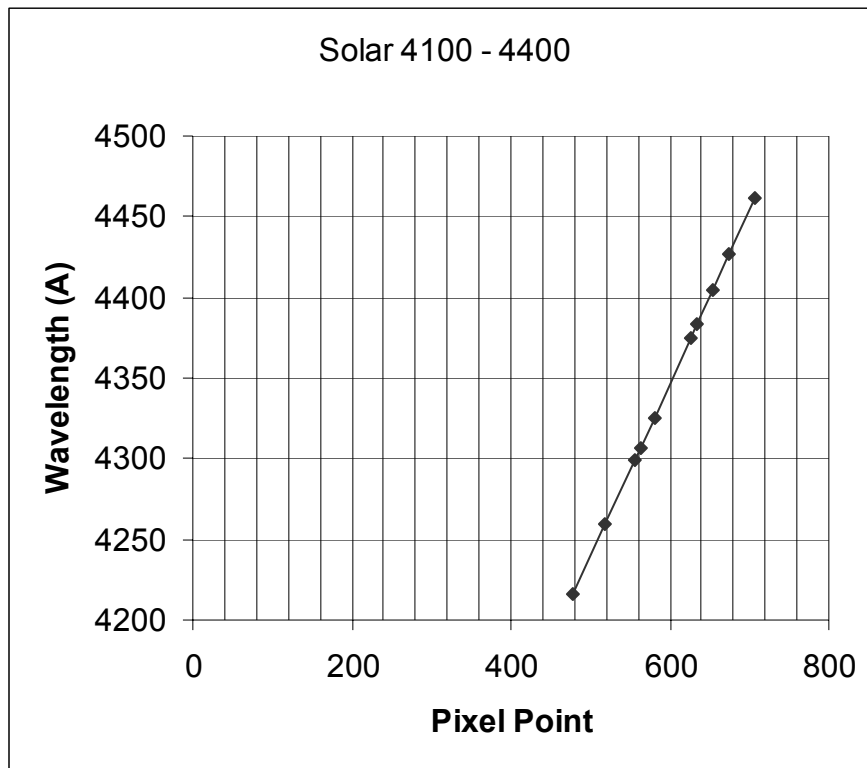


Figure 4.25 Graph of wavelength of reference lines vs pixel points (4100-4400 °A range)

Gradient (m) = 1.07  
 Interceptor (c) = 3704.5

Equation of straight line

$$Y = 1.07 X + 3704.5 \quad (4.7)$$

Table 4.16 Identified Absorption Lines of Spectrum ( 4100-4400 °A range) and Corresponding Elements.

| Pixel Point | Wavelength (°A) | Identified Elements | Intensity of the line |
|-------------|-----------------|---------------------|-----------------------|
| 463         | 4199.90         |                     |                       |
| 487         | 4225.59         | Ca (I)              | 1614 p                |
| 531         | 4272.67         |                     |                       |
| 557-569     | 4300-4313       | G band              |                       |
| 580         | 4325.00         | Fe                  | 2058 p                |
| 594         | 4340.00         | H $\gamma$          | 1949 p                |

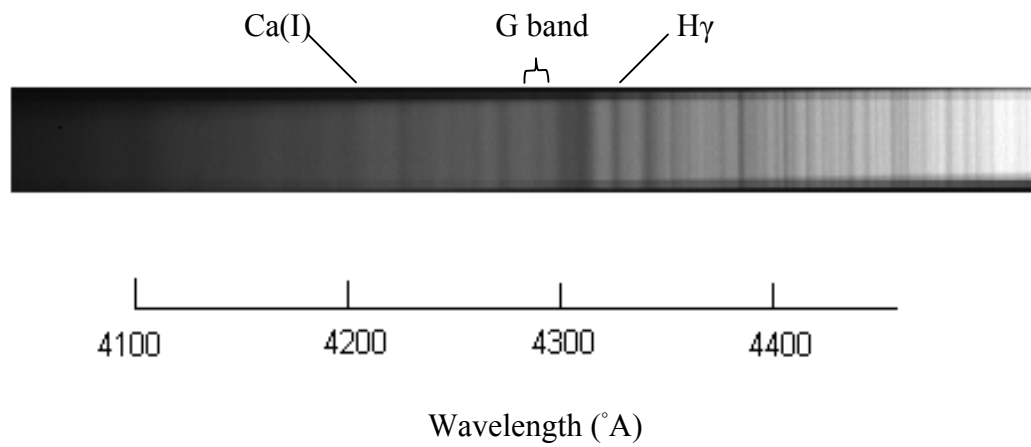


Figure 4.26 Absorption lines of elements ( 4100-4400 °A)

### 4.1.8 Solar Spectrum (4900 – 5700) °A

The Solar spectrum obtained at Grating Angle 46° of the Spectrograph.

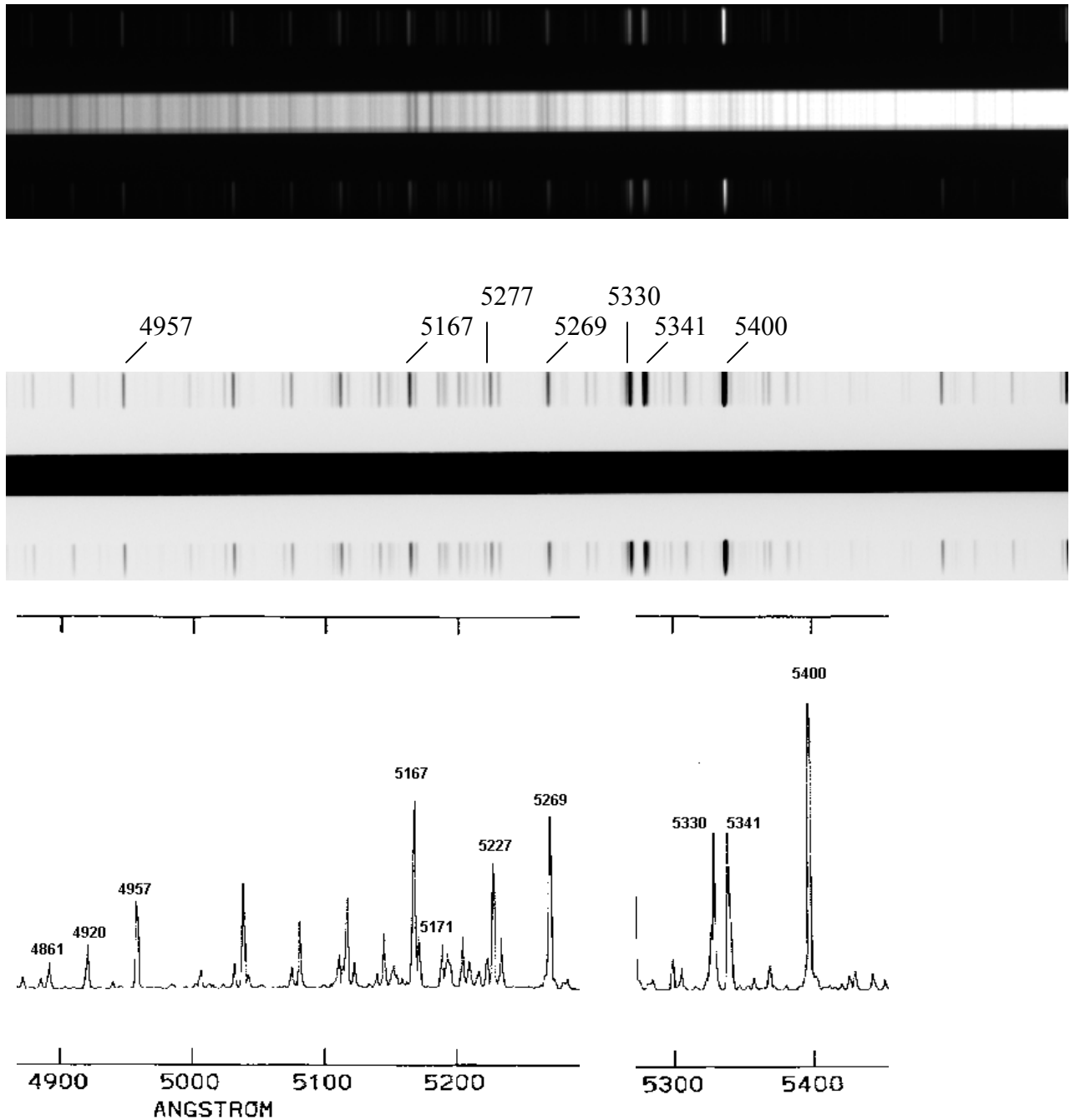


Figure 4.18 Reference line identification of range ( 4900-5700 °A)

Table 4.11 Pixel Points of Reference Lines ( 4900-5700 °A range)

| Wavelength (°A) | Pixel Point |
|-----------------|-------------|
| 4920            | 46          |
| 4957            | 80          |
| 5167            | 274         |
| 5227            | 329         |
| 5269            | 368         |
| 5330            | 424         |
| 5341            | 434         |
| 5400            | 487         |

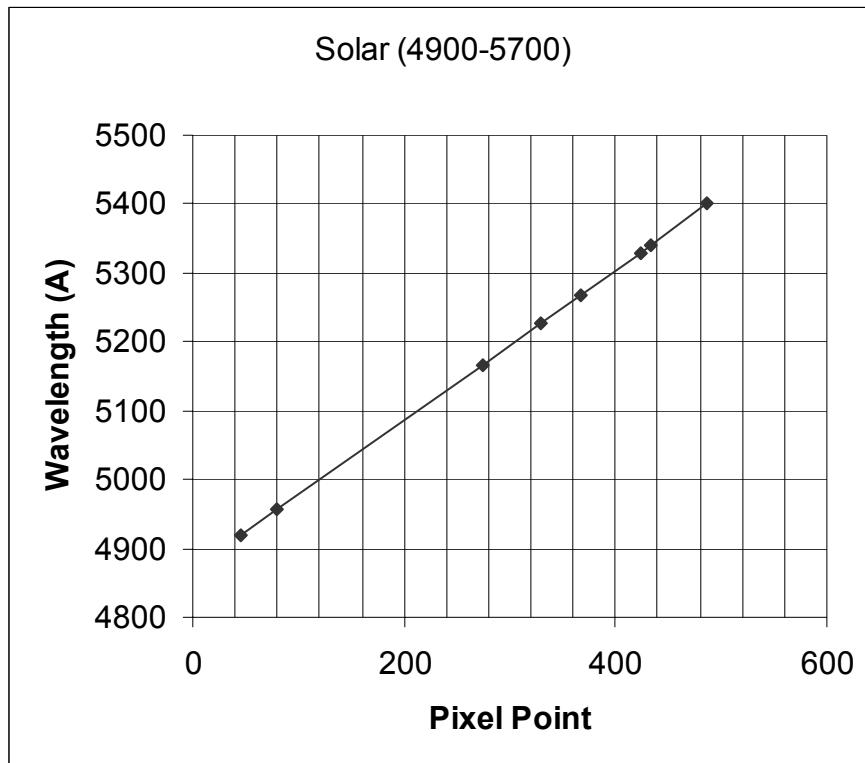


Figure 4.19 Graph of wavelength of reference lines vs pixel points (4900-5700 °A range)

Gradient (m) = 1.086

Interceptor (c) = 4870

Equation of the straight line

$$Y = 1.086 X + 4870 \quad (4.5)$$

Table 4.12 Identified Absorption Lines of Spectrum ( 4900-5700 °A range) and Correspond Elements.

| Pixel Point | Wavelength (°A) | Identified Elements | Intensity of the Line |
|-------------|-----------------|---------------------|-----------------------|
| 19          | 4890            | Fe                  | 9005 p                |
| 45          | 4919            | Fe                  | 9580 p                |
| 158         | 5042            | Fe                  | 10939 p               |
| 275         | 5169            | Mg                  | 10864 p               |
| 279         | 5173            | Mg                  | 9949 p                |
| 289         | 5184            | Mg                  | 9719 p                |
| 310         | 5207            | Cr                  | 14174                 |
| 329         | 5227            | Fe                  | 12899                 |
| 364         | 5265            | Mg                  | 13430                 |
| 368         | 5267            | Fe                  | 12702                 |
| 380         | 5283            | Fe                  | 15352                 |
| 394         | 5298            |                     |                       |
| 422         | 5328            | Fe                  | 14669                 |
| 461         | 5371            | Fe                  | 16279                 |
| 492         | 5404            | Fe                  | 16028                 |
| 520         | 5435            | Fe                  | 17981                 |
| 530         | 5446            | Fe                  | 17231                 |
| 538         | 5454            |                     |                       |
| 557         | 5475            | Ni                  | 17015                 |
| 604         | 5526            | Mg                  | 17916                 |
| 658         | 5585            |                     |                       |

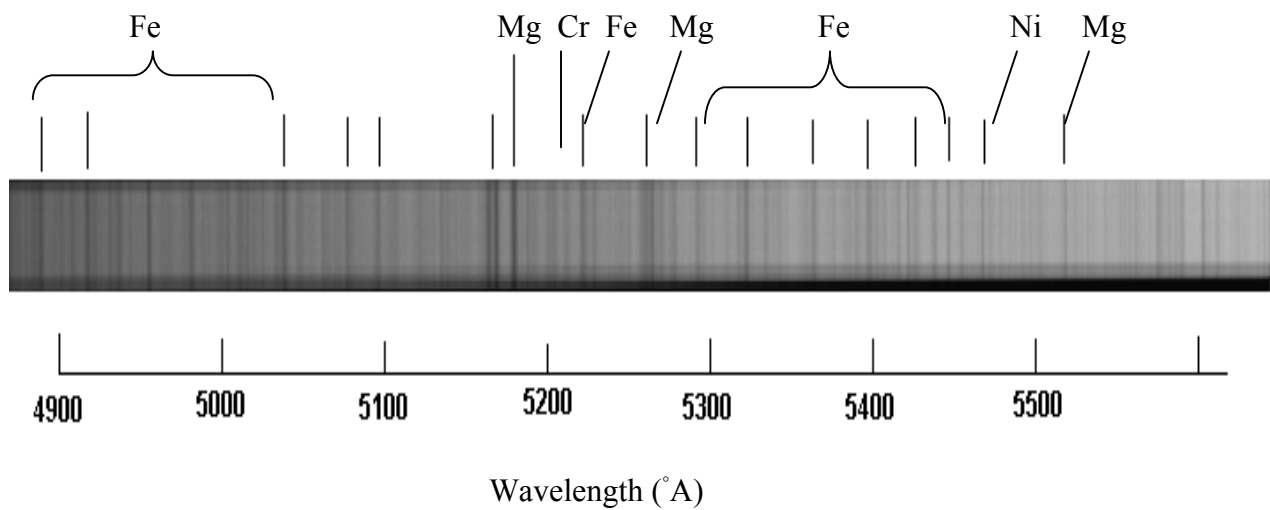


Figure 4.20 Absorption lines of elements ( 4900-5700 °A range)

## 4.2 Determination Solar Temperature Using Black Body Curve

The Black Body Radiation curve is valuable in astrophysics because it is a source of determination of many characteristics. The Black Body Radiation curve of certain object gives the wavelength of its maximum radiation. That is called  $\lambda_{\max}$ . The Win's Displacement Law gives the Temperature according to the equation.

$$\lambda_{\max} T = 0.2897 \quad \text{—————} \quad (4.2)$$

Where  $\lambda$  in centimeters  
T in Klvins

### 4.2.1 Identification of Intensities Distribution of entire Solar Spectrum

In order to plot the Black Body curve, the full range of the solar spectrum was obtained by changing the Grating angle of the spectrograph. These spectrums were taken under a bright sunny day at the same intensity condition as much as possible. The intensity along the spectrum is plotted using IRAF for entire range of solar spectrum. All intensity curves are attached as appendix A and an example is shown in figure 4.27

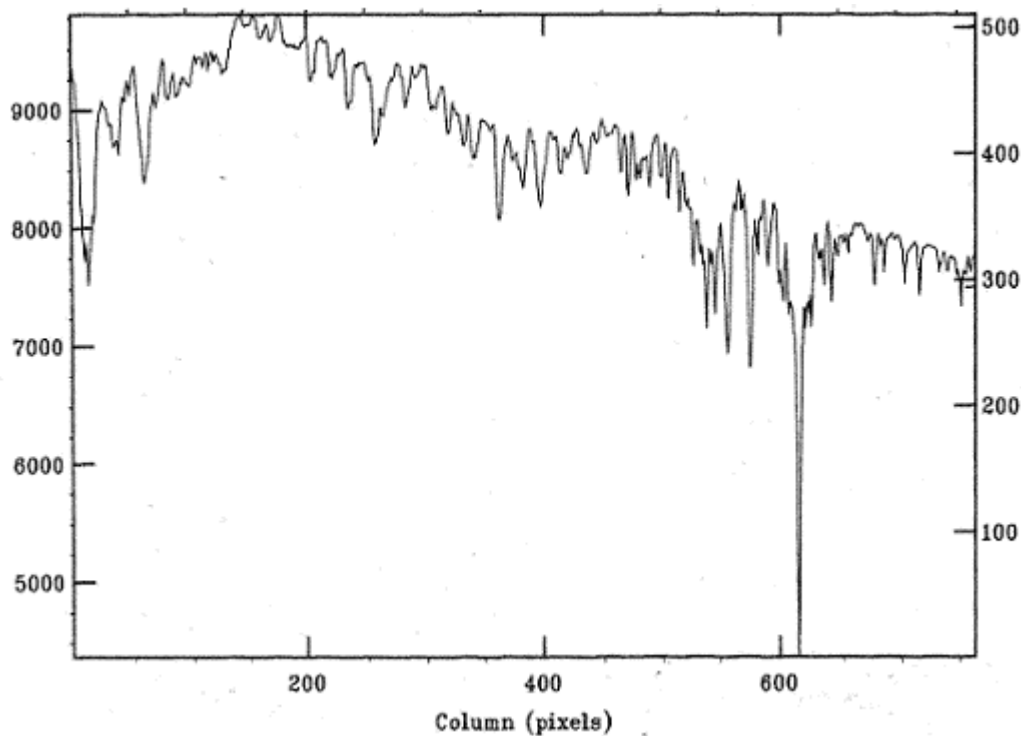


Figure 4.27 The Intensity Distribution of the Solar Spectra (range 5800-6700) given by IRAF. (Sixty lines were averaged and the grating angle was  $42^\circ$ )

Since there was absorption lines the intensity curve was disturbed as the sudden intensity drops (refer fig.4.27). The figure 4.27 shows the intensity vs pixel point. As in chapter 4.1 the wavelength corresponds to each pixel point was calculated using the reference lines of hollow cathode. The intensities were read out from these curves for selected pixel points. The table 4.17 shows the selected pixel points and corresponding read out intensities for the curve in figure 4.27

Table 4.17 The Pixel Points and Corresponding Intensities read out from the Intensity curve of range (5800 – 6700 °A)

| Pixel Point | Intensity |
|-------------|-----------|
| 0           | 9750      |
| 50          | 9500      |
| 100         | 9500      |
| 150         | 9750      |
| 200         | 9625      |
| 250         | 9500      |
| 300         | 9375      |
| 350         | 9125      |
| 400         | 9000      |
| 450         | 8875      |
| 500         | 8750      |
| 550         | 8625      |
| 600         | 8375      |
| 650         | 8250      |
| 700         | 8000      |
| 750         | 7750      |

The wavelengths for above pixel points are obtained by the calibration of the spectrum as the chapter 4.1 and those are wavelengths for the above intensities. This procedure was followed and calculated around ninety wavelengths and their intensities for the range of 3700 °A to 9000 °A.

#### 4.2.2 Quantum Correction of the Intensities.

There is a spectral response for every optical detector. i.e. they are impossible to response equally in all wavelengths. The Quantum Efficiency is the factor dealing with spectral response. The ST – 7 CCD camera was used for the project and the quantum efficiency of the camera is shown in the figure 2.5.

The figure 2.5 shows there is no equal response in the camera. There for the intensity correction must be done. According to the graph there is quantum efficiency for each wavelength. But it is impossible to find the quantum efficiency for single wavelength. There for quantum efficiency found for certain wavelength region using the above graph.

Table 4.18 Quantum Efficiency of Wavelength intervals for ST-7 CCD

| Wavelength Interval( $^{\circ}$ A) | Quantum Efficiency |
|------------------------------------|--------------------|
| 3750-4000                          | 0.2375             |
| 4250-4500                          | 0.2875             |
| 4500-4750                          | 0.3375             |
| 4750-5000                          | 0.3875             |
| 5000-5250                          | 0.3875             |
| 5250-5500                          | 0.3875             |
| 5500-5750                          | 0.4750             |
| 5750-6000                          | 0.5625             |
| 6000-6250                          | 0.6125             |
| 6250-6500                          | 0.6125             |
| 6500-6750                          | 0.5750             |
| 6750-7000                          | 0.5500             |
| 7000-7250                          | 0.5125             |
| 7250-7500                          | 0.4500             |
| 7500-7750                          | 0.4250             |
| 7750-8000                          | 0.4250             |
| 8000-8250                          | 0.3875             |
| 8250-8500                          | 0.3250             |
| 8500-8750                          | 0.3000             |
| 8750-9000                          | 0.2875             |
| 9000-9250                          | 0.2500             |
| 9250-9500                          | 0.2000             |
| 9500-9750                          | 0.1625             |
| 9750-10000                         | 0.1125             |

The corrected intensity for given wavelength is given by the equation

$$\text{Corrected Intensity} = \frac{\text{the intensity obtained from CCD for given wavelength}}{\text{the quantum efficiency of that wavelength}}$$

The intensities are corrected for all wavelengths and tabulated in table 4.19

### 4.2.3 Black Body Radiation Curve of Solar Radiation obtained before and after the Quantum Efficiency Correction

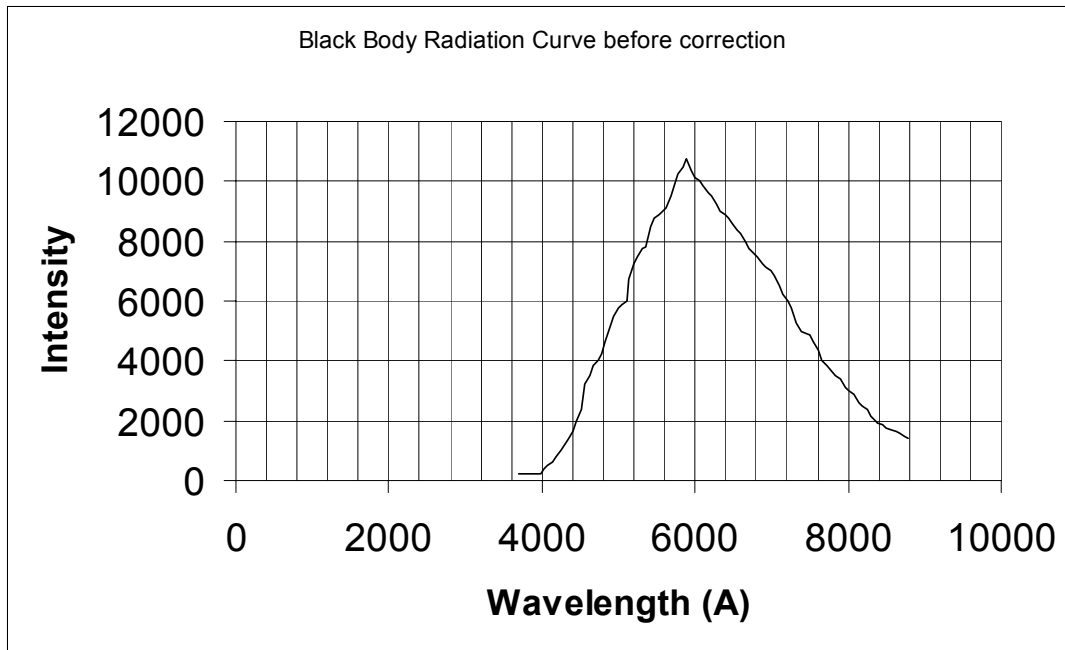


Figure 4.29 Black body radiation curve of sun before intensity correction

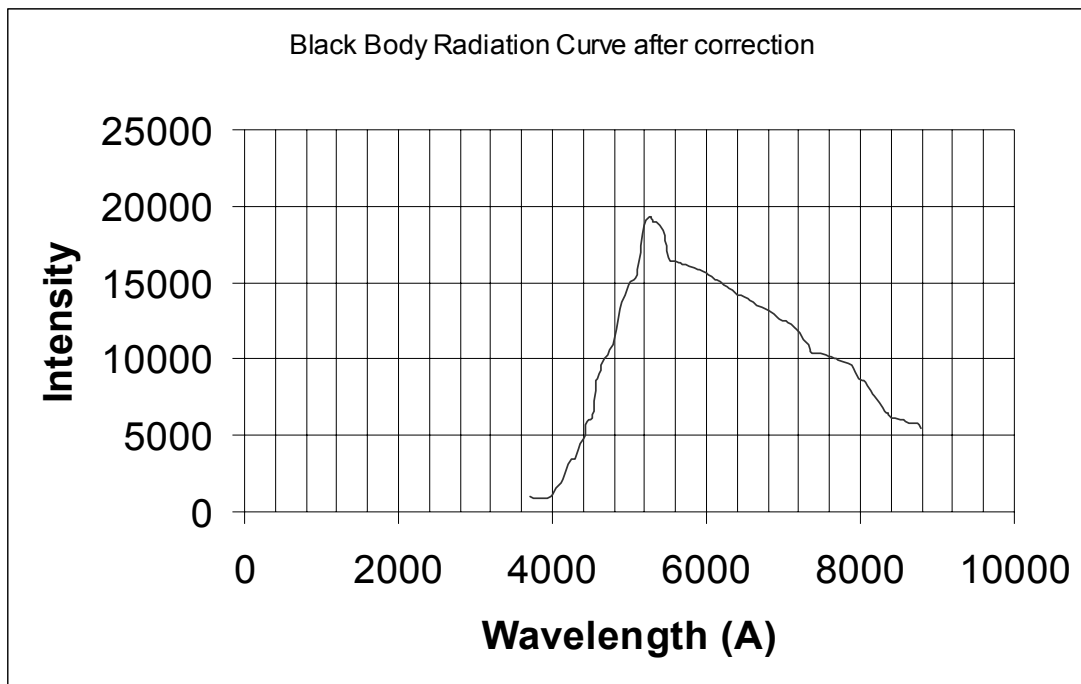


Figure 4.30 Black body radiation curve of the sun after intensity correction

#### 4.2.4 Solar Temperature

The value of  $\lambda_{\max}$  is read out from the corrected Black Body Radiation curve.

$$\begin{aligned}\lambda_{\max} &= 5250 \text{ \AA} \\ &= 5250 \times 10^{-8} \text{ cm}\end{aligned}$$

By equation 4.2

$$\lambda_{\max} \cdot T = 0.2897 \text{ cmK}$$

$$T = \frac{0.2897 \text{ cmK}}{5250 \times 10^{-8} \text{ cm}}$$

$$\underline{\underline{T = 5518 \text{ K}}}$$

## Chapter 5

### *Discussion*

The spectra consists almost all information about stars and stellar systems. A detail study of its spectral line indicates the temperature, pressure, receding or approaching speed of stars, chemical composition etc. The chemical composition of solar spectrum was analyzed to see whether what kind of elements or molecules does exist in the sun. Wavelengths of large number of absorption lines were recovered but it is impossible to find elements for each and every wavelength. The range of 4000 – 7000 °A of solar spectrum was examined and most prominent lines were recognized with the related elements. The identified elements are matched with the following solar spectrum analysis done by Mount Wilson Observatory<sup>1</sup>.

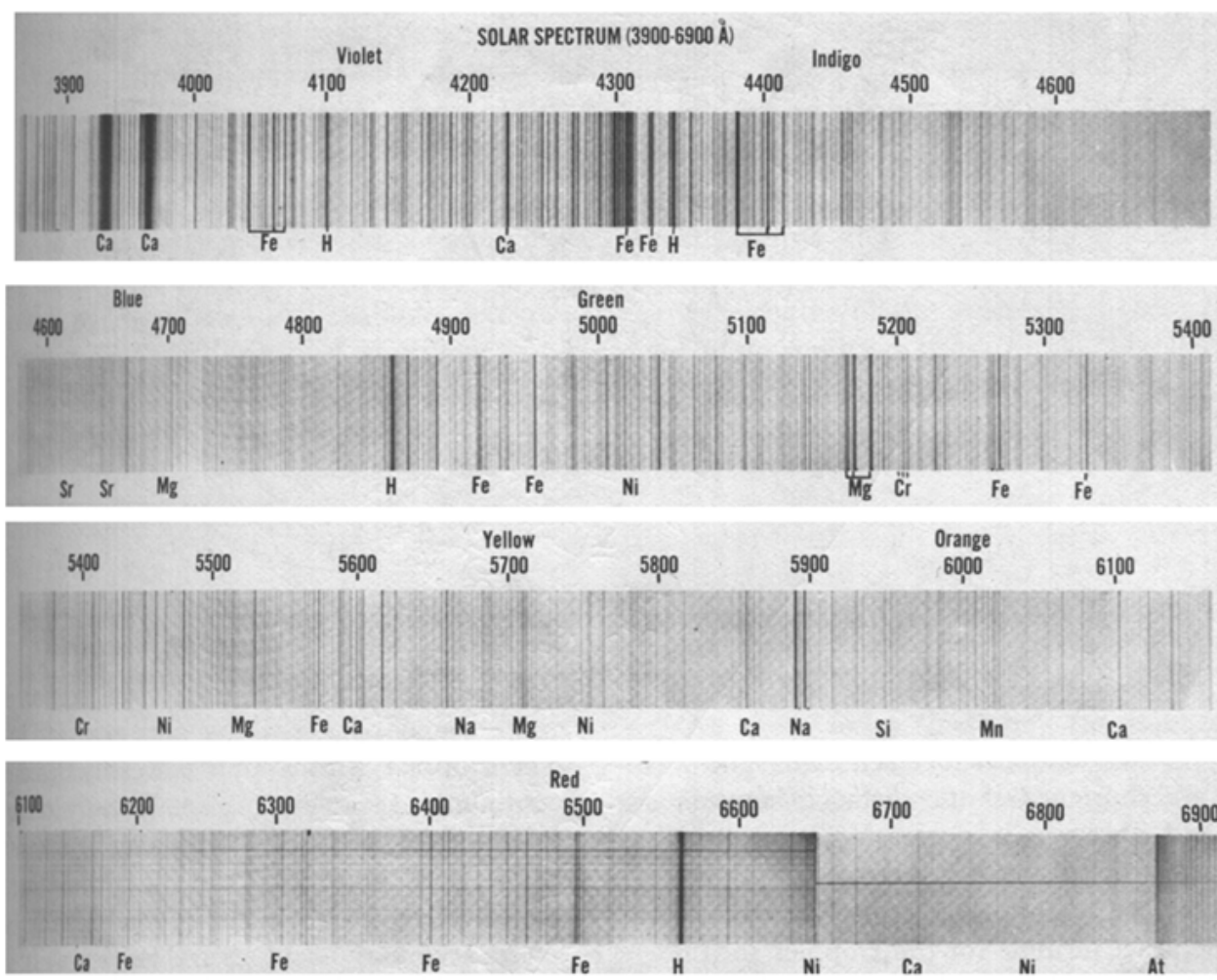


Figure 5.1 The Solar Spectrum Observed by Mount Wilson Observatory. Labels indicate the Elements in the Sun's Photosphere that causes some of dark lines. (Adapted from George O. A. 1982)

The similar elements have been identified in the present work as described under the data analysis chapter. Especially Hydrogen lines were identified with good accuracy.

|            |           |
|------------|-----------|
| H $\alpha$ | = 6563 °A |
| H $\beta$  | = 4861 °A |
| H $\gamma$ | = 4340 °A |
| H $\delta$ | = 4102 °A |

The H $\alpha$  line is the most prominent line of the spectra and conspicuity is less along the H $\alpha$  to H $\gamma$ . The H $\alpha$  is very sharp while H $\beta$  and H $\gamma$  are very faint. Although the Hydrogen lines can identify, the lines are weak relative to hot stars. The H $\delta$  line cannot find as it is close to the UV range. The solar temperature is not sufficient to give the strong lines of Hydrogen and Helium. This may be the reason for observing no He lines recognized in the entire range of solar spectra.

According to the observations of the whole spectrum there were weak few lines in the lower part (4000-5000 °A range) while there were many more strong lines in the higher wavelengths (6000-7000 °A range). The molecules and atmospheric absorption are responsible for this strong abundance of lines and they would not identify because of their line spectra wavelengths could not be found in data books.

In aid of absorption lines one can figure out the spectral category of a star. There are seven spectral types. O, B, A, F, G, K, & M. The each category can be separate into ten sub categories which are O1, O2, O3,.....O10. The solar spectrum has very weak He and H lines. The most of the solar spectrum consists of ionized metals. According to the spectral types shown in the fig.5.2 the sun belongs to G class where the hottest stars fell on the type O which has strong lines of ionized Helium.

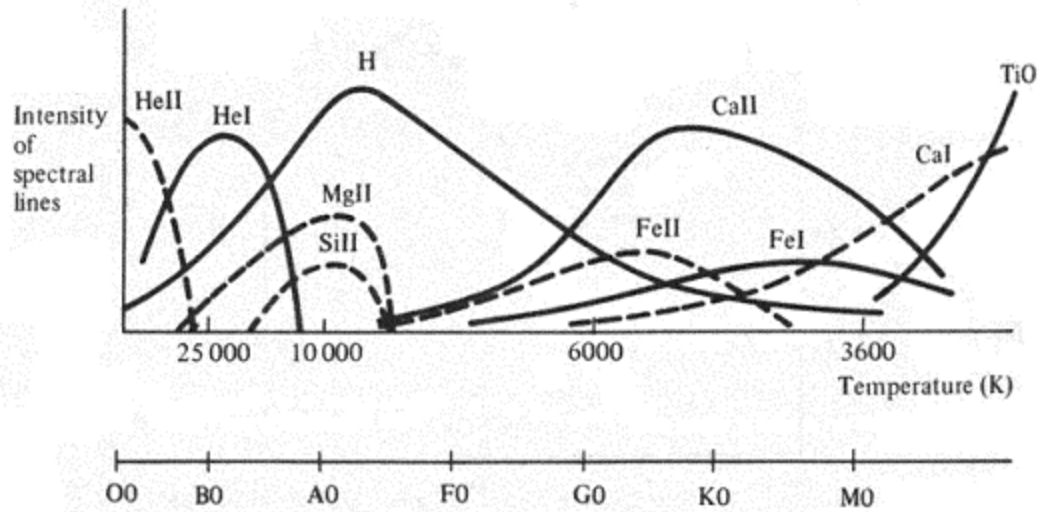


Figure 5.2 Temperature at which the absorption lines of some important atoms have there maximum intensity.(Adapted from Donald M. 1987)

The G-band (metal) and ionized Ca line are also recognized in the region of 4100-4400 °A. The conspicuous ionized Ca lines known as K and H are not found because the spectral response of CCD was not supporting less than 4000°A wavelengths. The quantum efficiency (see fig.2.5) of CCD is very low at smaller wavelengths and it was a limitation to observe lines like Ca in smaller wavelength region.

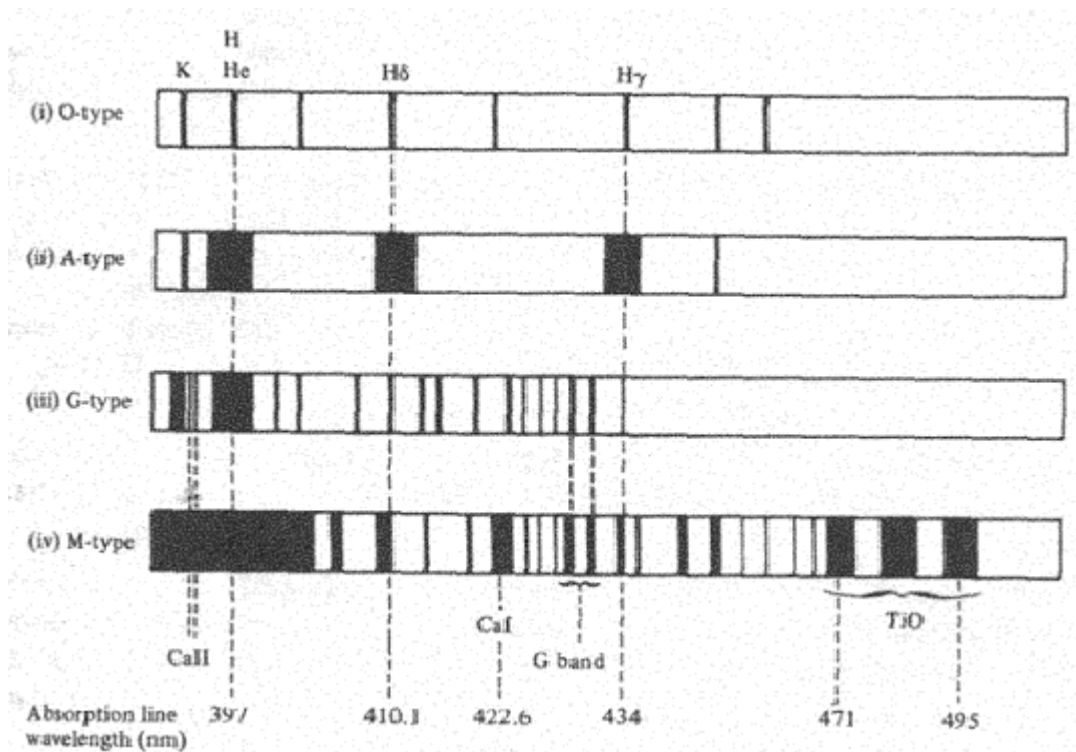


Figure 5.3 Ionized calcium lines and G-band of O, A, G, M type stars (Adapted from Donald, 1987)

The presence of few lines of same element provides the evidence that it occurs in the stellar medium. The solar spectrum consists of few Hydrogen lines and number of Iron lines. There for we can deduce that Hydrogen and Iron must be present in the solar outer layer. The Ca, Mg, Sr, Ni, Si, each has more than one line. Being identifying a single line we cannot presume that this element is present in the stellar medium. More than one line of particular element is necessary to say that it is a composition of the star. That determines the above elements are contributed to make the solar outer layer.

### Atmospheric Absorption of Radiation

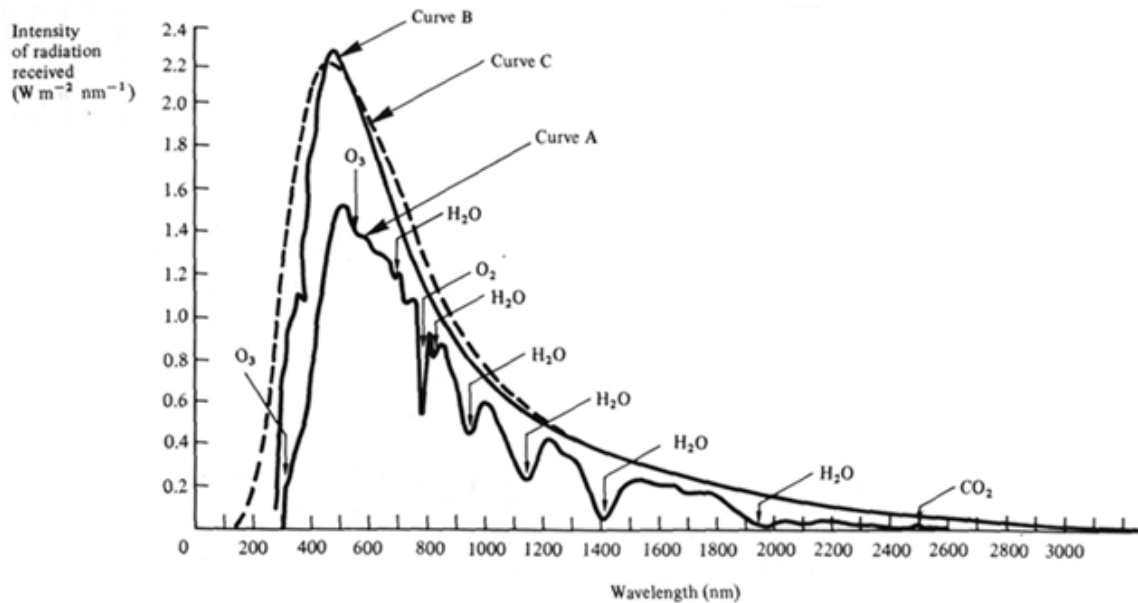


Figure 5.4 The effect of atmospheric absorption on the spectrum of the sun (Adapted from Donald, 1987)

In Fig. 5.4 the curve B show's the sun's energy spectrum when the observation made above the atmosphere. Curve C is the theoretical radiation curve for black body at 6000K. Curve A shows the sun's energy spectrum as recorded at the sea level. Most probably the atmospheric absorptions occur in the spectra as a band. The analysis found that there is an atmospheric absorption in the range of 7200-7600 °A. The very wide dark band present around 7600 °A (see Fig.4.8) in the observed spectra and also the above figure shows the prominent atmospheric absorption due to the O<sub>2</sub> in the range of 7600 °A.

## **Black Body Radiation Curve and Stellar Temperature.**

The Black Body Radiation curve is very vital in the study of stellar objects. The aim of plotting black body radiation curve is to determine solar temperature. Due to the abundance of absorption lines the intensity curves obtained from IRAF (see Fig.4.27) is not uniform. Therefore it is very hard to read out the accurate intensity value for a certain pixel point. Due to this inconvenient the black body radiation curve of the sun is not smooth one. Although it is not smooth the curve is sufficient to find  $\lambda_{\max}$  and hence the temperature.

The intensity correction is most important in the calculation. Before the intensity correction the  $\lambda_{\max}$  is 5891 Å. (refer table.4.19). Then the temperature is 4918 K. The temperature with the correction is 5518 K. The actual value of solar temperature is 5920K. There is a considerable deviation with the actual temperature before the correction. The corrected value is deviated but it is close to the real value. By looking at the two values it is clear the importance of the correction. The errors of the read out intensity values may be affected to the deviated solar temperature.

The intensity curves of the brightest star “Sirius” are obtained and shown on the appendix. The intensity curves are connected together and observe the pattern of the black body radiation curve of the Sirius.

There were numerous effects we have to consider under obtaining the image spectra, especially when the intensity has to be measured. The solar spectrum was taken from the reflected sunlight of white screen in order to maintain uniform intensity through out the experiment and also avoided the cloud cover of sunlight as much as possible. However the crystal clear sky is very rare in the urban areas. The clouds, dust, light pollution and bad weather are considerable obstacles. We cannot totally avoid these obstacles. Only thing is minimizing the obstacles and get the best data at the right time. Due to the lack of Astrophysics researches I had difficulties. But I am satisfied with my work.

## *Conclusion*

- A few prominent elements were recognized in the solar outer layer. The Hydrogen (H) and Iron (Fe) are there with the small amount of other elements Ca, Mg, Sr, Ni, Si, and Na.
- The elements identified in the sun using the spectrograph at the ACCIMT observatory are similar to those recorded at Mount Wilson Observatory. Therefore the methodology used here can be adapted for spectral observation of stars at the ACCIMT 45 cm reflective telescope.
- Identification of elements, temperature, and receding speeds of other stars too can be obtained using the same technique. But care should be taken to avoid the mass absorption due to the earth's atmosphere.
- The sun is not a hot star due to the weak Hydrogen lines detected in its spectrum. The experimentally obtained solar temperature was around 5500 K. This concludes that the sun is a type G star according to the spectral classification.
- The present location of the telescope in a light polluted environment hinders the accurate intensity observations of spectrums.

## ***Appendix A***

The Intensity Distribution of the entire Solar Spectrum and star Sirius.

## Appendix B

### The Line Spectra of Solar Elements

| Hydrogen        | Lithium         | Helium          | Carbon          | Sulfur          |
|-----------------|-----------------|-----------------|-----------------|-----------------|
| Wave length (Å) |
| 3970.07         | 4132.56         | 3964.73         | 3918.98         | 4120.8          |
| 4101.74         | 4132.62         | 4009.27         | 3920.69         | 4142.3          |
| 4340.47         | 4273.07         | 4026.19         | 4074.52         | 4145.1          |
| 4861.33         | 4273.13         | 4026.36         | 4075.85         | 4153.1          |
| 6562.72         | 4325.42         | 4120.82         | 4267.00         | 4162.7          |
| 6562.85         | 4325.47         | 4120.99         | 4267.26         | 4694.1          |
|                 | 4325.54         | 4143.76         | 4771.75         | 4695.4          |
|                 | 4602.83         | 4387.93         | 4932.05         | 4696.2          |
|                 | 4602.89         | 4437.55         | 5052.17         | 4716.2          |
|                 | 4671.65         | 4471.48         | 5132.94         | 4815.5          |
|                 | 4671.70         | 4471.68         | 5133.28         | 4924.1          |
|                 | 4678.06         | 4685.40         | 5143.49         | 4925.3          |
|                 | 4678.29         | 4685.70         | 5145.16         | 4993.5          |
|                 | 4881.32         | 4713.15         | 5151.09         | 5428.6          |
|                 | 4881.39         | 4713.38         | 5380.34         | 5432.8          |
|                 | 4881.49         | 4921.93         | 5648.07         | 5453.8          |
|                 | 4971.66         | 5015.68         | 5662.47         | 5473.6          |
|                 | 4971.75         | 5047.74         | 5889.77         | 5509.7          |
|                 | 5483.55         | 5411.52         | 5891.59         | 5564.9          |
|                 | 5485.65         | 5875.62         | 6001.13         | 5606.1          |
|                 | 6103.54         | 5875.97         | 6006.03         | 5640.0          |
|                 | 6103.65         | 6560.10         | 6007.18         | 5640.3          |
|                 | 6707.76         | 6678.15         | 6010.68         | 5647.0          |
|                 | 6707.91         | 6867.48         | 6013.22         | 5659.9          |
|                 |                 | 7065.19         | 6014.84         | 5664.7          |
|                 |                 | 7065.71         | 6578.05         | 5706.1          |
|                 |                 |                 | 6582.88         | 5819.2          |
|                 |                 |                 | 6587.61         | 6052.7          |
|                 |                 |                 | 6783.9          | 6286.4          |
|                 |                 |                 | 7113.18         | 6287.1          |
|                 |                 |                 | 7115.19         | 6305.5          |
|                 |                 |                 | 7115.63         | 6312.7          |
|                 |                 |                 | 7116.99         | 6384.9          |
|                 |                 |                 | 7119.90         | 6397.3          |
|                 |                 |                 |                 | 6398.0          |
|                 |                 |                 |                 | 6413.7          |
|                 |                 |                 |                 | 6743.6          |
|                 |                 |                 |                 | 6748.8          |
|                 |                 |                 |                 | 6757.2          |
|                 |                 |                 |                 | 7579.0          |

| Strontium       | Magnesium       | Neon            | Oxygen          |
|-----------------|-----------------|-----------------|-----------------|
| Wave length (Å) | Wave length (Å) | Wave length (Å) | Wave length (Å) |
| 4030.38         | 4054.69         | 4219.74         | 3911.96         |
| 4032.38         | 4057.50         | 4233.85         | 3919.29         |
| 4077.71         | 4075.06         | 4250.65         | 3947.29         |
| 4161.80         | 4081.83         | 4369.86         | 3947.48         |
| 4215.52         | 4165.10         | 4379.4          | 3947.59         |
| 4305.45         | 4167.27         | 4379.55         | 3954.37         |
| 4438.04         | 4351.91         | 4385.06         | 3954.61         |
| 4607.33         | 4354.53         | 4391.99         | 3973.26         |
| 4722.28         | 4380.38         | 4397.99         | 3982.20         |
| 4741.92         | 4384.64         | 4409.30         | 4069.90         |
| 4784.32         | 4390.59         | 4413.22         | 4072.16         |
| 4811.88         | 4428.00         | 4421.39         | 4075.87         |
| 4832.08         | 4433.99         | 4428.52         | 4083.91         |
| 4855.04         | 4436.49         | 4428.63         | 4087.14         |
| 4868.70         | 4436.60         | 4430.9          | 4089.27         |
| 4872.49         | 4481.16         | 4430.94         | 4097.24         |
| 4876.06         | 4481.33         | 4457.05         | 4105.00         |
| 4876.32         | 4534.29         | 4522.72         | 4119.22         |
| 4891.98         | 4571.10         | 4537.75         | 4132.81         |
| 4962.26         | 4621.30         | 4540.38         | 4146.06         |
| 4967.94         | 4702.99         | 4569.06         | 4153.30         |
| 5156.07         | 4730.03         | 4704.40         | 4185.46         |
| 5222.20         | 4739.59         | 4708.86         | 4189.79         |
| 5225.11         | 4739.71         | 4710.07         | 4233.27         |
| 5229.27         | 4851.10         | 4712.07         | 4253.74         |
| 5238.55         | 5167.33         | 4715.35         | 4253.98         |
| 5256.90         | 5172.68         | 4752.73         | 4275.47         |
| 5329.82         | 5183.61         | 4788.93         | 4303.78         |
| 5450.84         | 5264.21         | 4790.22         | 4317.14         |
| 5480.84         | 5264.37         | 4827.34         | 4336.86         |
| 5486.12         | 5345.98         | 4884.92         | 4345.56         |
| 5504.17         | 5401.54         | 5005.16         | 4349.43         |
| 5521.83         | 5509.60         | 5037.75         | 4366.90         |
| 5534.81         | 5528.41         | 5144.94         | 4368.25         |
| 5540.05         | 5711.09         | 5330.78         | 4395.95         |
| 5543.36         | 5785.31         | 5341.09         | 4414.91         |
| 5970.10         | 5785.56         | 5343.28         | 4416.98         |
| 6345.75         | 5916.43         | 5400.56         | 4448.21         |
| 6363.94         | 5918.16         | 5562.77         | 4452.38         |
| 6369.96         | 6318.72         | 5656.66         | 4465.45         |
| 6380.75         | 6319.24         | 5719.23         | 4466.28         |
| 6386.50         | 6319.49         | 5748.30         | 4467.83         |
| 6388.24         | 6346.74         | 5764.42         | 4469.41         |
| 6408.47         | 6346.96         | 5804.45         | 4590.97         |

| Strontium       | Magnesium       | Neon            | Oxygen          |
|-----------------|-----------------|-----------------|-----------------|
| Wave length (Å) | Wave length (Å) | Wave length (Å) | Wave length (Å) |
| 6446.68         | 6545.97         | 5820.16         | 4596.17         |
| 6465.79         | 6620.44         | 5852.49         | 4609.39         |
| 6504            | 6620.57         | 5872.83         | 4638.85         |
| 6546.79         | 6630.83         | 5881.9          | 4641.81         |
| 6550.26         | 6781.45         | 5902.46         | 4649.14         |
| 6617.26         | 6787.85         | 5906.43         | 4650.84         |
| 6643.54         | 6812.86         | 5944.83         | 4661.64         |
| 6791.05         | 6819.27         | 5965.47         | 4676.23         |
| 6878.38         | 6894.9          | 5974.63         | 4699.21         |
| 6892.59         | 6965.4          | 5975.53         | 4705.36         |
|                 | 7060.41         | 5987.91         | 4924.6          |
|                 |                 | 6030            | 4943.06         |
|                 |                 | 6074.34         | 5329.1          |
|                 |                 | 6096.16         | 5329.68         |
|                 |                 | 6128.45         | 5330.74         |
|                 |                 | 6143.06         | 5435.18         |
|                 |                 | 6163.59         | 5435.78         |
|                 |                 | 6182.15         | 5436.86         |
|                 |                 | 6217.28         | 5577.34         |
|                 |                 | 6266.5          | 5958.39         |
|                 |                 | 6304.79         | 5958.58         |
|                 |                 | 6334.43         | 5995.28         |
|                 |                 | 6382.99         | 6046.23         |
|                 |                 | 6402.25         | 6046.44         |
|                 |                 | 6506.53         | 6046.49         |
|                 |                 | 6532.88         | 6106.27         |
|                 |                 | 6598.95         | 6155.98         |
|                 |                 | 6652.09         | 6156.77         |
|                 |                 | 6678.28         | 6158.18         |
|                 |                 | 6717.04         | 6256.83         |
|                 |                 | 6929.47         | 6261.55         |
|                 |                 | 7024.05         | 6366.34         |
|                 |                 | 7032.41         | 6374.32         |
|                 |                 | 7051.29         | 6453.6          |
|                 |                 | 7059.11         | 6454.44         |
|                 |                 |                 | 6455.98         |
|                 |                 |                 | 6604.91         |
|                 |                 |                 | 6653.83         |
|                 |                 |                 | 7001.92         |
|                 |                 |                 | 7002.23         |
|                 |                 |                 | 7156.7          |

| Barium          | Calcium         | Nitrogen        | Silicon         |
|-----------------|-----------------|-----------------|-----------------|
| Wave length (Å) | Wave length (Å) | Wave length (Å) | Wave length (Å) |
| 4036.26         | 3923.48         | 3919            | 4102.94         |
| 4083.77         | 3933.66         | 3955.85         | 4128.07         |
| 4084.86         | 3935.29         | 3995            | 4130.89         |
| 4130.66         | 3946.04         | 4035.08         | 4183.35         |
| 4132.43         | 3948.9          | 4041.31         | 4190.72         |
| 4166            | 3957.05         | 4043.53         | 4198.13         |
| 4216.04         | 3968.47         | 4099.94         | 4621.42         |
| 4267.95         | 3972.57         | 4109.95         | 4621.72         |
| 4283.1          | 3973.71         | 4176.16         | 4782.99         |
| 4287.8          | 4097.1          | 4227.74         | 4792.21         |
| 4297.6          | 4098.53         | 4236.91         | 4792.32         |
| 4309.32         | 4098.57         | 4237.05         | 4883.2          |
| 4323            | 4109.82         | 4241.78         | 4906.99         |
| 4325.73         | 4110.28         | 4432.74         | 4932.8          |
| 4326.74         | 4206.18         | 4447.03         | 4947.61         |
| 4329.62         | 4220.07         | 4530.41         | 5006.06         |
| 4350.33         | 4226.73         | 4601.48         | 5041.03         |
| 4402.54         | 4240.46         | 4607.16         | 5055.98         |
| 4405.23         | 4283.01         | 4613.87         | 5181.9          |
| 4431.89         | 4289.36         | 4621.39         | 5185.25         |
| 4488.98         | 4298.99         | 4630.54         | 5192.86         |
| 4493.64         | 4302.53         | 4643.08         | 5202.41         |
| 4505.92         | 4307.74         | 4788.13         | 5295.19         |
| 4509.63         | 4318.65         | 4803.29         | 5405.34         |
| 4523.17         | 4355.08         | 4847.38         | 5417.24         |
| 4524.93         | 4425.44         | 4895.11         | 5428.92         |
| 4554.03         | 4434.96         | 4914.94         | 5432.89         |
| 4573.85         | 4435.69         | 4935.12         | 5438.62         |
| 4579.64         | 4454.78         | 4950.23         | 5447.26         |
| 4599.75         | 4455.89         | 4963.98         | 5454.49         |
| 4619.92         | 4456.61         | 4987.37         | 5456.45         |
| 4628.33         | 4472.04         | 4994.36         | 5466.43         |
| 4644.1          | 4479.23         | 5001.48         | 5466.87         |
| 4673.62         | 4489.18         | 5002.7          | 5469.21         |
| 4691.62         | 4526.94         | 5005.15         | 5493.23         |
| 4700.43         | 4578.55         | 5007.32         | 5496.45         |
| 4708.94         | 4581.4          | 5010.62         | 5517.54         |
| 4726.44         | 4581.47         | 5016.39         | 5540.74         |
| 4843.46         | 4585.87         | 5025.66         | 5576.66         |
| 4847.14         | 4585.96         | 5045.1          | 5622.22         |

| Barium          | Calcium         | Nitrogen       | Silicon         |
|-----------------|-----------------|----------------|-----------------|
| Wave length (Å) | Wave length (Å) | Wave length(Å) | Wave length (Å) |
| 4850.84         | 4685.27         | 5281.2         | 5632.97         |
| 4877.65         | 4716.74         | 5292.68        | 5639.48         |
| 4899.97         | 4721.03         | 5495.67        | 5645.61         |
| 4902.9          | 4799.97         | 5535.36        | 5660.66         |
| 4934.09         | 4878.13         | 5666.63        | 5665.55         |
| 4947.35         | 5001.48         | 5676.02        | 5669.56         |
| 4957.15         | 5019.97         | 5679.56        | 5681.44         |
| 4997.81         | 5021.14         | 5686.21        | 5684.48         |
| 5013            | 5041.62         | 5710.77        | 5688.81         |
| 5159.94         | 5188.85         | 5747.3         | 5690.43         |
| 5267.03         | 5261.71         | 5752.5         | 5701.11         |
| 5361.35         | 5262.24         | 5764.75        | 5701.37         |
| 5391.6          | 5264.24         | 5829.54        | 5706.37         |
| 5421.05         | 5265.56         | 5854.04        | 5708.4          |
| 5424.55         | 5270.27         | 5927.81        | 5747.67         |
| 5428.79         | 5285.27         | 5931.78        | 5753.63         |
| 5480.3          | 5307.22         | 5940.24        | 5754.22         |
| 5519.05         | 5339.19         | 5941.65        | 5762.98         |
| 5535.48         | 5349.47         | 5952.39        | 5772.15         |
| 5620.4          | 5512.98         | 5999.43        | 5780.38         |
| 5680.18         | 5581.97         | 6008.47        | 5785.73         |
| 5777.62         | 5588.76         | 6167.76        | 5793.07         |
| 5784.18         | 5590.12         | 6379.62        | 5794.9          |
| 5800.23         | 5594.47         | 6411.65        | 5797.86         |
| 5805.69         | 5598.49         | 6420.64        | 5800.47         |
| 5826.28         | 5601.29         | 6423.02        | 5806.74         |
| 5853.68         | 5602.85         | 6428.32        | 5827.8          |
| 5907.64         | 5857.45         | 6437.68        | 5846.13         |
| 5971.7          | 5922.72         | 6440.94        | 5867.48         |
| 5981.25         | 5923.69         | 6457.9         | 5868.4          |
| 5997.09         | 6102.72         | 6468.44        | 5873.76         |
| 5999.85         | 6122.22         | 6482.05        | 5915.22         |
| 6019.47         | 6161.29         | 6482.7         | 5948.55         |
| 6063.12         | 6162.17         | 6483.75        | 5957.56         |
| 6110.78         | 6163.76         | 6481.71        | 5978.93         |
| 6135.83         | 6166.44         | 6484.8         | 6067.45         |
| 6141.72         | 6169.06         | 6491.22        | 6080.06         |
| 6341.68         | 6169.56         | 6499.54        | 6086.67         |
| 6378.91         | 6439.07         | 6506.31        | 6125.02         |
| 6450.85         | 6449.81         | 6610.56        | 6131.57         |

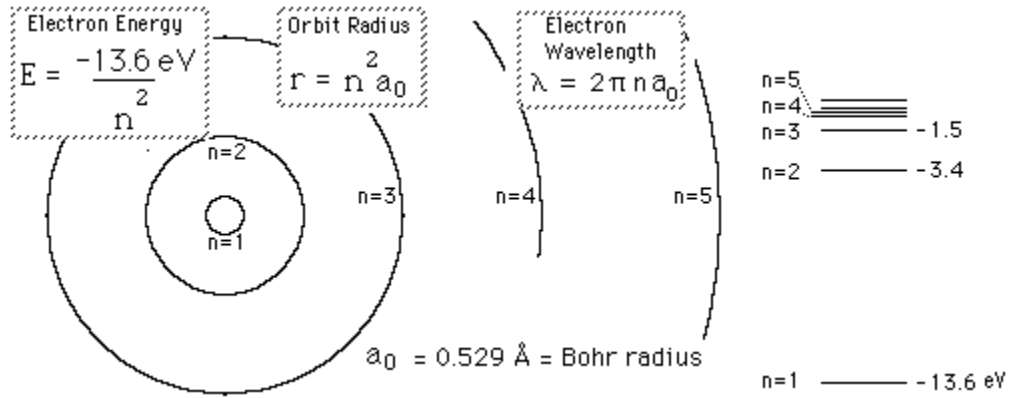
| Barium          | Calcium         | Nitrogen        | Silicon         |
|-----------------|-----------------|-----------------|-----------------|
| Wave length (Å) | Wave length (Å) | Wave length (Å) | Wave length (Å) |
| 6482.91         | 6455.6          | 6622.54         | 6131.85         |
| 6496.9          | 6456.87         | 6636.94         | 6142.49         |
| 6498.76         | 6462.57         | 6644.96         | 6145.02         |
| 6527.31         | 6471.66         | 6646.5          | 6155.13         |
| 6595.33         | 6493.78         | 6653.46         | 6237.32         |
| 6654.1          | 6499.65         | 6656.51         | 6238.29         |
| 6675.27         | 6572.78         | 6722.62         | 6243.81         |
| 6693.84         | 6717.69         |                 | 6244.47         |
| 6769.62         | 7148.15         |                 | 6254.19         |
| 6865.69         |                 |                 | 6331.95         |
| 6867.85         |                 |                 | 6347.1          |
| 6874.09         |                 |                 | 6371.36         |
|                 |                 |                 | 6526.61         |
|                 |                 |                 | 6527.2          |
|                 |                 |                 | 6555.46         |
|                 |                 |                 | 6660.52         |
|                 |                 |                 | 6665            |
|                 |                 |                 | 6671.88         |
|                 |                 |                 | 6699.38         |
|                 |                 |                 | 6717.04         |
|                 |                 |                 | 6721.85         |
|                 |                 |                 | 6741.64         |
|                 |                 |                 | 6750.28         |
|                 |                 |                 | 6818.45         |
|                 |                 |                 | 6829.82         |
|                 |                 |                 | 6848.57         |
|                 |                 |                 | 6976.52         |
|                 |                 |                 | 7003.57         |
|                 |                 |                 | 7005.88         |
|                 |                 |                 | 7017.28         |
|                 |                 |                 | 7017.65         |
|                 |                 |                 | 7034.9          |
|                 |                 |                 | 7164.69         |
|                 |                 |                 | 7165.55         |
|                 |                 |                 | 7184.89         |
|                 |                 |                 | 7193.58         |
|                 |                 |                 | 7193.9          |

| Iron            |                 |                 |                 |                |
|-----------------|-----------------|-----------------|-----------------|----------------|
| Wave length (Å) | Wave length (Å) | Wave length (Å) | Wave length (Å) | Wave length(Å) |
| 4005.24         | 4216.18         | 4872.14         | 5232.94         | 5569.62        |
| 4009.71         | 4219.36         | 4878.21         | 5260.26         | 5572.84        |
| 4014.53         | 4222.21         | 4890.75         | 5266.56         | 5586.76        |
| 4021.87         | 4225.96         | 4891.49         | 5269.54         | 5615.64        |
| 4040.64         | 4227.42         | 4903.31         | 5270.36         | 5624.54        |
| 4045.81         | 4233.6          | 4918.99         | 5281.79         | 5662.52        |
| 4063.59         | 4235.94         | 4920.5          | 5283.62         | 5762.99        |
| 4066.98         | 4238.8          | 4957.6          | 5302.3          | 5862.35        |
| 4067.98         | 4247.43         | 5001.86         | 5324.18         | 5914.11        |
| 4071.74         | 4250.12         | 5001.91         | 5328.04         | 5986.96        |
| 4076.63         | 4250.79         | 5005.71         | 5328.53         | 5961.71        |
| 4100.74         | 4258.32         | 5006.12         | 5332.9          | 5962.4         |
| 4107.49         | 4260.47         | 5012.07         | 5339.93         | 6065.48        |
| 4118.54         | 4271.15         | 5014.94         | 5341.02         | 6102.16        |
| 4127.6          | 4271.76         | 5030.77         | 5364.87         | 6136.61        |
| 4132.06         | 4282.4          | 5041.76         | 5367.47         | 6137.69        |
| 4134.68         | 4291.46         | 5049.82         | 5369.96         | 6147.73        |
| 4137            | 4299.23         | 5051.63         | 5371.49         | 6149.24        |
| 4143.42         | 4307.9          | 5074.75         | 5383.37         | 6191.56        |
| 4143.87         | 4315.08         | 5100.73         | 5393.17         | 6213.43        |
| 4153.9          | 4325.76         | 5110.36         | 5397.13         | 6219.28        |
| 4154.5          | 4352.73         | 5133.69         | 5404.12         | 6230.73        |
| 4156.8          | 4369.77         | 5139.25         | 5405.77         | 6238.37        |
| 4172.74         | 4375.93         | 5139.46         | 5410.91         | 6246.32        |
| 4174.91         | 4383.54         | 5151.91         | 5415.2          | 6247.56        |
| 4175.64         | 4404.75         | 5162.27         | 5424.07         | 6252.55        |
| 4177.59         | 4415.12         | 5166.28         | 5427.83         | 6393.6         |
| 4181.75         | 4427.3          | 5167.49         | 5429.7          | 6400           |
| 4184.89         | 4461.65         | 5168.89         | 5434.52         | 6411.65        |
| 4187.04         | 4466.55         | 5171.6          | 5446.87         | 6416.9         |
| 4187.8          | 4476.02         | 5191.45         | 5455.45         | 6421.35        |
| 4191.43         | 4482.17         | 5192.34         | 5455.61         | 6430.84        |
| 4195.32         | 4482.25         | 5194.94         | 5465.93         | 6446.43        |
| 4198.3          | 4489.74         | 5204.58         | 5466.94         | 6456.38        |
| 4199.1          | 4528.61         | 5215.18         | 5482.31         | 6494.98        |
| 4202.03         | 4647.43         | 5216.27         | 5497.52         | 6516.05        |
| 4203.98         | 4736.77         | 5216.85         | 5501.46         | 6546.24        |
| 4206.7          | 4859.74         | 5226.86         | 5506.2          | 6592.91        |
| 4210.34         | 4871.32         | 5227.15         | 5506.78         | 6677.99        |

## Appendix C

### Mechanism of producing emission spectra of elements using Hydrogen atom.

The basic Hydrogen energy level structure in the agreement with the Bohr model is shown in the following figure. Each main shell associated with a value of the principle quantum number  $n$ .

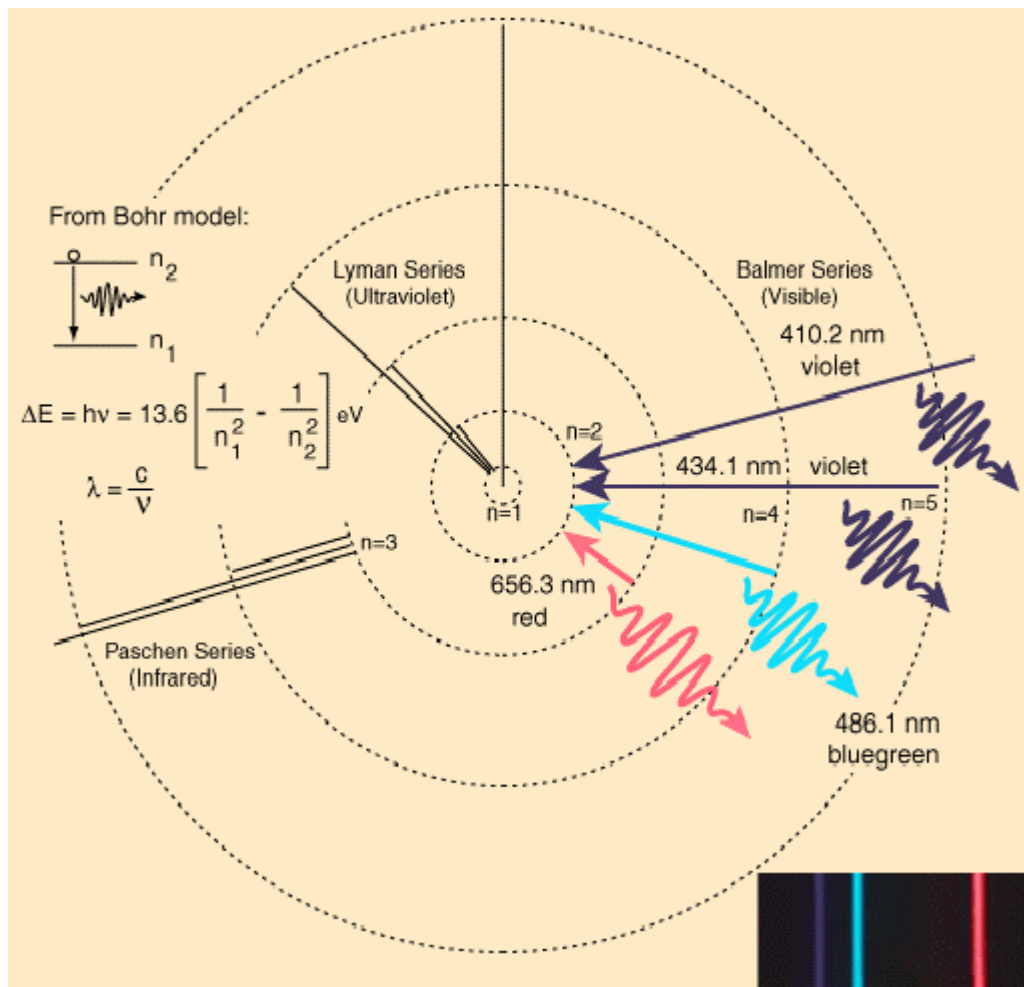


The electrons in the main shells are excited when energy absorption is occurred. After a short interval the electron drops back down to its ground state, with simultaneous emission of energy. The emission energy is given by the equation C1.

$$h\nu = \frac{2\pi^2me^4}{h^2} \left[ \frac{1}{n_1^2} - \frac{1}{n_2^2} \right] \quad \text{———— C1}$$

This energy is emitted as light causing emission line spectra of elements.





The emission line spectra of Hydrogen atom.

## **List of Reference**

1. GEORGE, O.A. (1982). *Exploration of the Universe, 4<sup>th</sup> ed.* pp 161-212, pp 400-427, CBS College Publishing (Winston)
2. DONALD, M. (1987). *Physics and Astronomy*, pp 87-128, Macmillan Press LTD (London)
3. RICHARD, B., Terry, D. (1984). *Astrophysics I, Stars*, pp 2-138, Jones and Bartlett Publishers (Boston)
4. ERIKA, B., VITENSE. (1989). *Introduction to Stellar Astrophysics, Volume 1*, pp 1-100, Cambridge University Press (London).
5. PASACHOFF, M. (1991). *Astronomy from the Earth to the Universe, 4<sup>th</sup> ed.* pp 330-350, Saunders College Publishing (Winston).
6. DAVID, R. L. (2000). *CRC Hand Book of Chemistry and Physics (2000-2001), 81<sup>st</sup> ed.* pp 10-1 to 10-88, Chemical Rubber Publishing.
7. MODEL ST-7 CCD *camera operating manual*. Santa Barbara Instrument Group.

## **Web Sites**

8. WWW. *Sbgi.com*
9. Http. *Iraf.noao.edu*
10. WWW. *Nasa.gov*



